AMMONIA AND ACETIC ACID INHIBITIONS IN ANAEROBIC DIGESTION

AMMONIA AND ACETIC ACID INHIBITIONS IN ANAEROBIC DIGESTION

By: SARAH FERNANDES, B.Eng.

A Thesis Submitted to the School of Graduate Studies

in Partial Fulfilment of the Requirements for the Degree of

Master of Applied Science

McMaster University MASTER OF APPLIED SCIENCE (2020) Hamilton, Ontario (Civil Engineering)

TITLE: Ammonia and Acetic Acid Inhibitions in Anaerobic Digestion

AUTHOR: Sarah Fernandes, B.Eng (McMaster University)

SUPERVISOR: Dr. Younggy Kim

NUMBER OF PAGES: ix, 72

Abstract

Anaerobic Digestion (AD) is an essential component in wastewater treatment to recover energy from waste and deals with sludge management issues effectively. AD is a treatment process that converts organic matter to methane and carbon dioxide with multi-step biological reactions. Methanogenesis, the subprocess of AD that produces methane, is an important indicator of the stability of AD and is influenced by pH, temperature, ammonia, volatile fatty acids (VFAs), and solids concentrations among other factors.

Ammonia is an essential nutrient for methanogenic bacteria but at certain ammonia concentrations and pH levels, ammonia is said to be a toxicant for methanogenic archaea. Substrates that are high in ammonia content can include those high in protein, such as food waste, which can be inhibitory to methanogens in the digestion process. Thickened waste activated sludge (TWAS) also contains a large amount of nitrogen with its higher solids concentration, promoting methane production. VFAs are produced during acidogenesis and they can negatively affect methanogenic archaea. High organic loading rates into AD can lead to an accumulation of VFAs and thus inhibition of methanogenic activity. Even with well-known inhibitory effects of ammonia and VFAs on methanogenesis, there are limited tools available for modelling these inhibitions, especially when evaluating diverse compositions of substrate. The objectives of this research work are to experiment for various pairings of pH, ammonia, and acetate levels using batch reactors and to quantify the inhibition on the overall methane production using an AD-based model focused on biological reactions.

Acknowledgments

To have so many people in my life who support, challenge, and believe in me is a blessing. I am appreciative of:

My supervisor, Dr. Younggy Kim, for the opportunity to learn and grow under your supervision. I am grateful for all the time, guidance, and advice you provided at every step of my academic career. I would not have been able to achieve this milestone without everything you have taught me and all our discussions about water treatment.

My committee members, Dr. Yiping Guo and Youngseck Hong, for your time in reviewing and providing insightful criticisms to help me improve my work. Rajeev Goel and Spencer Snowling, for offering support and opportunities to present my research to you and to also gain feedback and appreciation for this work. Monica Han, for your dedication to the lab and availability for any help, questions, or discussions.

The support from NSERC Discovery Grants and DAS, ORF-RE and SOWC-AWT.

All my McMaster friends, particularly those in the Kim Lab and JHE 330, for providing helpful and sunny perspectives in windowless rooms. Robert, for an endless supply of computers and bad AD puns, ensuring I achieve my goals while enjoying the process. My fortunate circumstances to pursue a higher level of education in Canada could not have been possible without the motivation and support from my parents, Mary and Antonio (MNPW). I am forever grateful to all the educators, family, and friends that have supported me in this endeavour.

Table of Contents

List of Figures

List of Tables

List of Abbreviations

AD	Anaerobic digestion
ADM1	Anaerobic Digestion Model No. 1
BMP	Biochemical methane potential
CAS	Conventional activated sludge
COD	Chemical oxygen demand (g-COD/L)
FAN	Free ammonia-nitrogen (NH_3-N)
LCFA	Long chain fatty acid
SCFA	Short chain fatty acid
sCOD	Soluble chemical oxygen demand (g-COD/L)
TAN	Total ammonia-nitrogen (g-N/L)
TS/TSS	Total (suspended) solids (g-T(S)S/L)
(T)WAS	(Thickened) waste activated sludge
VBA	Visual basic application
VFA	Volatile fatty acids
VS/VSS	Volatile (suspended) solids (g-V(S)S/L)
WWTP	Wastewater treatment plant

1 Introduction

1.1 Anaerobic Digestion

1.1.1 Anaerobic Digestion Background

Anaerobic digestion (AD) is the decomposition of organic waste by anaerobic microorganisms in the presence of heat and with the absence of oxygen. The primary use of the anaerobic digestion process was to reduce odour and the mass of sludge for disposal at waste management sites. It has since been recognized for its use in sludge stabilization and as an appropriate technology to use for biosolids waste management given the limited environmental impacts and energy recovery potentials. Biogas, a renewable methane source and main ingredient in natural gas, is produced through biological treatment of wastes and wastewaters with different characteristics [1]. Regarding the municipal wastewater treatment process, AD by-products include biogas, which is theoretically composed of about 70% methane and 30% carbon dioxide, and digestate, which is the nutrient-rich sludge output that includes nitrogen and phosphorus [2]. The main goals of AD include inactivation of human pathogens, volatile solids reduction, volatile fatty acids stabilization, and stable methane production.

Within the municipal wastewater treatment process, influent is commonly treated using the conventional activated sludge (CAS) process which produces waste activated sludge (WAS) as a by-product. Based on the CAS process, WAS is composed of either primarily particulate organics or microorganisms. The biological reactions that govern the AD process are dependent on key factors like temperature and solid retention times. AD is typically operated under mesophilic (35 – 40 ºC) or thermophilic (50 – 55 ºC) temperatures [2]. While higher temperatures can enable better AD processing, the energy requirement

for operation of AD can be substantial due to the associated heating costs [3]. Typical anaerobic digesters require a minimum retention time of 15 days while 20 – 25 days is more common to ensure the retention of essential microorganisms [2]. Due to digester capacities, longer solids retention times are unfavourable and typically correlate to lower temperatures.

The use of AD for other biomass such as manure and food waste has been of interest in the waste management field to avoid landfilling [4]. Food waste can reduce the municipal solid waste fraction of organics for disposal and offers a method to reclaim the potential energy in the waste where nutrients can be recycled through land applications [5]. Notable food waste characteristics include slightly increased total solid, organic, and ammonia concentrations compared to that of WAS in municipal wastewater. A commonly used process within AD for such complex biomass is co-digestion, in which WAS is mixed with the food waste and digested together. This method is a form of process intensification as it reduces stress for certain microorganisms through digestion of a diverse substrate composition [6]. WAS typically has low organic concentrations while food waste is usually characterized by high nitrogen and carbon concentrations. Thus, most of the problems can be solved by anaerobic co-digestion with enhanced substrate providing a more balanced C/N ratio and a larger readily biodegradable organic fraction [3]. Co-digestion would also allow for more control over organic overloading and increase methane production.

Direct disposal methods such as landfilling and incineration were commonly used sludge management methods. Neither strategy is a viable solution given the costs involved with the transportation of WAS and the increasing production rates [7]. The environmental

impact associated with direct landfilling is also severely harmful given the volume of greenhouse gases that are produced from the organic conversions through sludge breakdown [8]. Thus, research into optimization of the AD process through the development of treatment technologies and process configurations continues to be a necessity. Research focusing on the effects of operational and environmental parameters are commonly studied in both academia and industry, including process parameters such as performance, stability, inhibition, toxicity, and process optimization [8]. At the industry level, most research development opportunities include reactor designs, separation technologies, process control and monitoring, and rate enhancement. Academic research focuses more into process and rate enhancement opportunities with performance stabilization, and process optimization by looking into specific biological reactions and microorganisms [8].

The necessity for AD is an idea that has spread globally and locally as AD is a proven technology with more than a hundred facilities in operation within Canada itself [1]. Some Canadian provinces have already banned food and organic waste from being discarded in landfills and incinerators for waste management, due to their harmful environmental impacts, with Ontario to start phasing-in this action in 2022 [9]. Thus, there are many incentives to improve the system using technologies that reduce the amount of inhibition and toxicity in the AD process and aid with increased biogas generation and solids reduction.

1.1.2 Biological Reactions in Anaerobic Digestion

AD is the process of stabilizing sludge by converting organics to biogas. The conversion of this sludge is based on multiple biological reactions that can be seen in three main steps: hydrolysis, acidogenesis/acetogenesis, and methanogenesis (Figure 1.1). All reactions occur in their specified order but also simultaneously as the conversion rates of each individual component are dependent on other components, boundary conditions, and operational parameters.

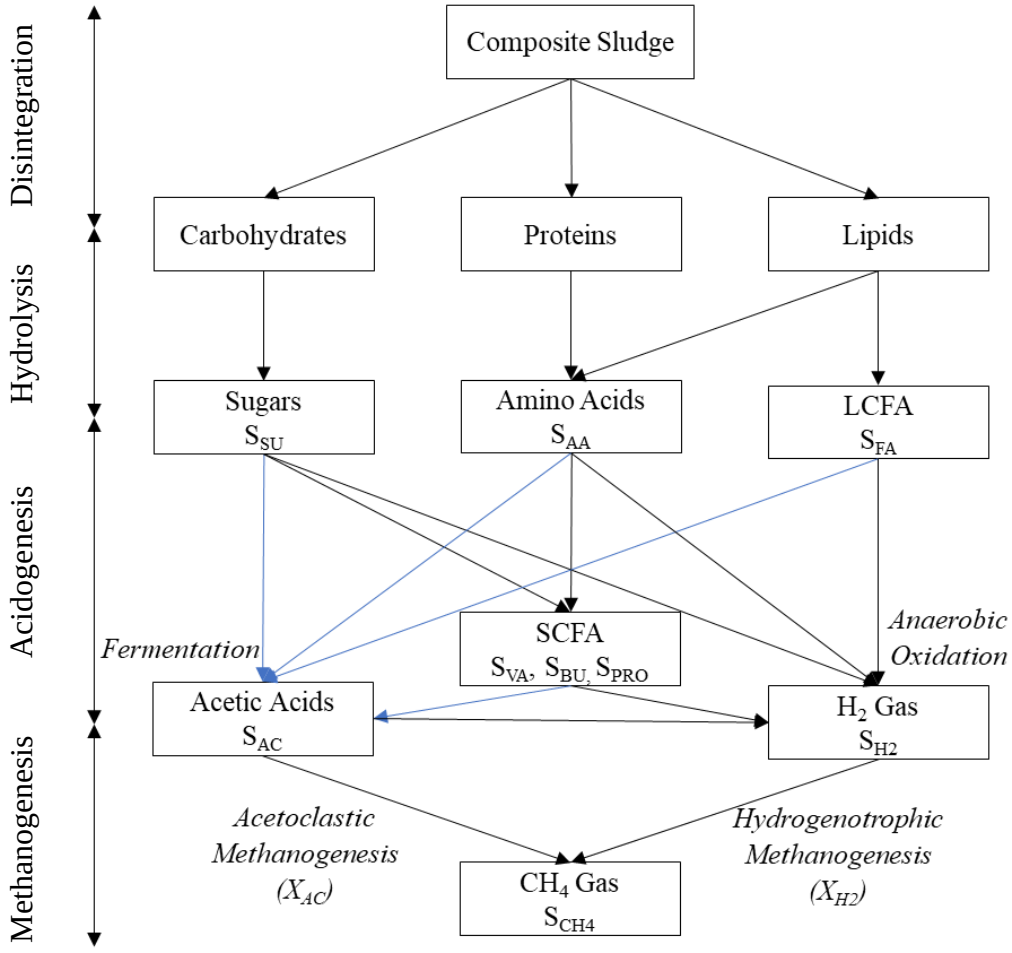

Figure 1.1: Anaerobic Digestion Process Diagram with ADM1 characterization.

The influent, WAS, is the sludge collected from clarifiers in the conventional activated sludge systems that is composed of particulate organics with WAS from secondary clarifiers being more difficult to breakdown. A polymer network of filamentous bacteria composed of proteins and polysaccharides clusters the organic content of WAS which enables biomass flocs to form and settle in the secondary clarifier [10]. The networks build up nutrient concentrations for bacteria feed while also protecting these microorganisms, but the disintegration of this network is important for dewatering of sludge and for accessing organics in WAS. This lack of accessibility is a limiting factor in AD [2]. The disintegration of this composite sludge produces biodegradable organics and inert inorganic material which is just the initial breakdown of the bulk sludge into particulate organic components for hydrolysis.

Hydrolysis is the first step of AD that breaks down particulate organics into soluble substrate. Hydrolysis transforms carbohydrates, proteins, and fats into sugars, amino acids, and long chain fatty acids. Ammonia-nitrogen is also released during hydrolysis as it is essential for the growth of anaerobic microorganisms at low concentrations. It is within this subprocess of AD where the breakdown of proteins causes undesirably high concentrations of ammonium [8]. Due to this breakdown of particulate organics, the fraction of particulate COD (pCOD) decreases as soluble COD (sCOD) increases [2]. Decomposition of organic compounds like carbohydrates leads to the increase of sCOD and volatile fatty acids (VFA) attributed by hydrolysing and fermentative bacteria. The rate of hydrolysis is dependent on the complexity of substrate composition and operational conditions which can make this subprocess rate limiting.

These soluble organic molecules are then converted to hydrogen gas and short chain fatty acids (SCFA) in acidogenesis. Fermentation of sugars and amino acids by acidogenesis produce VFAs, hydrogen, and carbon dioxide with the fastest reactions. Anaerobic oxidation of fatty acids (lipids, propionate, butyrate, and valerate) by acetogenesis produce acetate, carbon dioxide, and hydrogen. The VFAs are used as a carbon source for the diverse acetogenic microorganisms with this beta oxidation reaction. This subprocess of AD is susceptible to low pH issues if the amount of alkalinity is insufficient for the VFA production which leads to reductions in microorganism activity for the digester [2].

Finally, methanogenesis is the process in which methane is produced and is variable in its influence. Acetate, hydrogen, and carbon dioxide produced by acidogenesis are used for the organic source by the methanogenic microorganisms for biogas production. The two types of methanogens follow either the acetate pathway (for acetoclastic methanogens) or the hydrogen pathway (for hydrogenotrophic methanogens). Their individual roles convert their counter parts into methane but are of different characteristics and perform differently under changing AD conditions. Hydrogenotrophic methanogens are comprised of diverse and robust species that are not as susceptible to operational changes in pH conditions. Acetoclastic methanogens contribute about 70% of the methane production but are comprised of strict anaerobes that grow very slowly and are not remarkably diverse. Methanosaeta species are observed as the most abundant in seed sludge but decrease with increased acetate concentrations while Methanosarcina was determined to be the most abundant, regardless of operating temperatures [11]. In regards to ammonia concentrations,

it has been reported that acetate utilizing bacteria was affected by ammonia concentrations citing sensitivity to pH as a big factor, however, little is seen for the effect of hydrogenotrophic methanogens [11]. Methanogenesis is where inhibition is best observed as methane production is a main by-product of the AD process. The sludge by-product also evaluates the effectiveness of AD in sludge reduction of organics (COD).

1.2 Literature Review: Ammonia Inhibition in Anaerobic Digestion

Inhibitors commonly present in AD processes include ammonia and organics and due to the differences in the type and composition of wastes, inoculum, and experimental methods and conditions, literature results on inhibition for specific toxicants vary widely [12]. Food waste and livestock manure are similar in their composition with the high concentrations of ammonia. Compared to WAS, food waste has a higher solids concentrations at 3-10%, increased VS/TS ratios of 70-90%, and elevated ammonia concentrations from 0.9 – 6 g/L [13, 14]. Temperature, pH, VFA, and ammonia are the key environmental factors that influence the methanogenic pathway, showing inhibition.

Ammonia is an essential nutrient for bacterial growth and is produced by the degradation of nitrogenous matter [12]. The mechanisms suggested for ammonia inhibition have been implemented to deal with the change in cell pH, increased energy requirements for reactions, and inhibition of specific enzyme reactions. Inorganic ammonia nitrogen is present as the ammonium ion and free ammonia in aqueous solutions as shown in the dissociation equation, Eq. (1.1):

(pKa = 9.24) $$NH_4^+ \rightleftharpoons NH_3 + H^+ \quad (1.1)$$

Free ammonia-nitrogen (FAN) is commonly observed to be the main cause of inhibition as it is membrane-permeable and the hydrophobicity of the molecule would allow for passive diffusion into bacteria cells [12]. FAN is dependent on the total ammonia nitrogen concentration (TAN), pH, and temperature as shown in Eq. (1.2):

$$FAN = TAN * \frac{1}{1 + 10^{0.09018 + \frac{2729.92}{273.2+T} - pH}} \quad (1.2)$$

The concentration of ammonia can be quantitatively determined by the stoichiometric relationship between the anaerobic biodegradation of organic substrate to methane, carbon dioxide and ammonia. It is generally believed that ammonia concentrations can be beneficial to AD if less than 0.2 g-N/L, providing the necessary inorganic nitrogen nutrient concentration [12]. However, for most WAS compositions in municipal wastewater treatment, concentrations over 3 g-N/L have been regarded as the upper limit for non-inhibitory TAN concentrations while for high solids sludge [10, 15]. The pH affects the growth of microorganisms with high concentrations of TAN and with FAN being the predominantly toxic form of ammonia, increased pH conditions results in increased FAN and toxicity. Neutral pH conditions (7.0 ± 0.5) are necessary for most AD process stability factors but is demanded for by the moderate-high pKa value of ammonia [16]. Temperature can also influence inhibition as studies on cattle manure have observed inhibitory TAN concentrations at higher concentrations of 4 g-N/L with stable digestion up to 6 g-N/L at all pH levels with thermophilic digestion [17].

While FAN is seen as the main toxicant for ammonia inhibition, the ammonia ion is also thought to cause inhibition. Increased initial TAN concentrations at neutral pH

conditions have a dominant ammonium concentration and still pose an inhibition issue as the hydrolysis subprocess breaks down the particulate monomers into soluble components, increasing concentrations and toxicity effects [8]. Accumulation of the toxicants occurs during hydrolysis and can pose the inhibition issues based on TAN concentrations. The mechanism by which inhibition for ammonium occurs is based on the cellular distribution and allowance of diffusion of pH [18]. While the TAN concentration highly influences the effect of inhibition, pH and temperature are also very influential factors.

The pH and temperature determine the rate of methanogenesis produced by methanogens. This shift in pH leads to process instability with the toxic effect of FAN on methanogens that often results in acetate accumulation [8, 18]. This build-up inhibits the acetogenic steps and leads to the accumulation of propionate and butyrate. This VFA accumulation in turn further inhibits hydrolysis, decreases pH, and reduces the concentration of FAN. As free ammonia is the inhibition parameter, the decrease in the concentration stabilizes the process to still yield a lower amount of methane at a certain VFA and pH concentration for that AD composition, dependent on experimental and operational conditions [3]. Overall, compilations of these pH, temperature, and substrate factors have suggested varying TAN concentrations with a strong suggestion that substrates with lower organic concentrations have lower critical TAN concentrations and are therefore more susceptible to ammonia inhibition issues [8, 12, 17, 18, 19, 20]. Most studies believe that ammonia inhibition results from the acetogenic methanogenesis pathway as there is little inhibition for hydrogenotrophic bacteria [21]. This idea also stems

on the suspicion that FAN is the sole toxic agent responsible for any form of ammonia inhibition.

Inhibition affects reactor operations in AD by promoting reactor failure and thus economic loss ensues. Co-digestion has been an innovative process enhancement operation that is used to mitigate inhibitory effects with substrates and has been studied thoroughly. Another mitigation technique is to observe the seed usage rather than substrate. Acclimation of certain archaea to higher TAN concentrations has been seen to increase bacterial tolerance and mitigate some of the issues surrounding methane production as levels up to 5 g-N/L were seen to be tolerated with WAS and 3 g-N/L in piggery manure [22, 23].

1.3 Literature Review: Acetic Acid Inhibition in Anaerobic Digestion

Acetic acid is one of the components considered in the acidogenesis step of anaerobic digestion and together with other volatile fatty acids (VFA), is an important intermediate for methanogenesis. VFAs include, acetic acid, butyric acid, propionic acid, isobutyric acid, and isovaleric acid with acetic acid contributing more than 70% to methane production. VFAs are good indicators for monitoring AD performance in the activity of methanogenic microorganisms. Methanogenesis from acetate can come from acetoclastic and syntrophic acetate oxidation pathways with the latter pathway having a two-step oxidation and methanogenesis reaction.

The accumulation of acetate and higher VFA is the most noticeable result of an unstable AD process. Rapid failure is observed in most models when VFA concentration

increases past a threshold level or when pH decreases [24]. While pH is not observed to change drastically with most AD substrate, other factors such as high organic content with low alkalinity can push a digester towards instability as exemplified by dissociation equation, Eq (1.3):

(pKa = 4.78) $$CH_3COOH \rightleftharpoons CH_3COO^- + H^+$$ (1.3)

High VFA concentrations are commonly based on acetate accumulation which is a result of excessive ammonia concentrations inhibiting the acetogenesis and methanogenesis reactions. As this issue is common with individual TWAS and food waste substrate, it is often mitigated with process enhancement techniques such as the co-digestion of the two substrates. Acetate concentrations above ~4.3 g-COD/L have decreased acetoclastic methanogenesis and 13 g-COD/L of acetate contributed to over 50% inhibition [25].

The impact ammonia inhibition has on the degradation of acetic acid is studied and included in basic AD models while its effect on the degradation propionic and butyric acid is not considered. Inhibition of acetogenesis in AD is widely accepted that acetic acid accumulation leads to change in pH and inhibition of the cell activity whereas inhibition of acetogenesis might cause the accumulation of propionic and butyric acid [26]. Butyrate and propionate directly affect acetate which would mean acetate accumulation would affect these VFAs. Propionate accumulation was stated not to effect hydrogenotrophic methanogens, even with increased ammonia concentrations [27].

1.4 Literature Review: Anaerobic Digestion Model No. 1 (ADM1)

Anaerobic Digestion Model No. 1 (ADM1) is one of the most comprehensive AD models developed by the IWA task group as this model is structured to reflect the main biochemical steps, ion behaviour, gas-liquid transfer, mixing, mass transfer, and heat transfer through the use of biological, physico-chemical, and transport dynamic equations [28]. The biological processes convert complex organics into methane and carbon dioxide by-products and all components and processes can be seen in Figure 1.1 and Table 3.3. From its publication in 2002, ADM1 has been the starting point for many other anaerobic digestion models and has since been enhanced for different specifications. Industry has a great demand for a comprehensive AD model and has since implemented and developed software with the use of ADM1 and other models.

The original version of ADM1 looks at the 24 biochemical rate equations (7 biomass groups, 12 soluble compounds, and 5 particulate compounds) in conjunction with 19 biochemical kinetic processes, 7 physico-chemical equilibrium processes, and 3 gas-liquid mass transfer processes [28]. Simplification methodologies have been useful in developing more manageable models that still maintain equivocal simulation accuracy. A review on the history of AD modelling has shown that most models have differences in regards to the number of biomass groups, the number of steps within hydrolysis and methanogenesis, the form of inhibition functions used, the inclusion of physico-chemical processes and/or transport dynamics, and the characterization of substrate that is specified to WAS or generalized to simple fractionation of biochemical compounds. ADM1 was specifically developed for general modelling of AD, leaving open choices for the

implementation as opposed to the Activated Sludge Models which were more strictly designed for wastewater treatment [29].

Conversion of substrate processes in ADM1 are described by kinetic expressions dependent on the substrate concentration and rate constants. First order rate expressions are used in the hydrolysis and methanogenesis steps. Monod growth kinetic expressions with pH inhibition and non-competitive inhibition by VFA, free ammonia and hydrogen are typically used in the acidogenesis, acetogenesis and methanogenesis steps.

Analysis of kinetics in ADM1 has been focused on hydrogen inhibition with the non-competitive function. Some critical analysis suggests replacing this inhibition function with one dependent on free energy as a thermodynamic function [29]. The empirical formula used for pH inhibition has also been criticized as it is enabled for fermentative and methanogenic bacteria only for lower pH conditions. Ammonia inhibition is another key parameter that has had many inputs into its functionality as it is displayed as an inhibition of FAN solely with effects on the acetogenic pathway for methane production. However, this has since been widely disputed with alternative inhibition parameters that look at high pH inhibitions and both FAN and ammonium inhibition functions. Acetic acid inhibition parameters have not been considered in the generic ADM1 model but there have also been many suggestions towards its implementation in the model [30].

Along with the use of kinetics and inhibition equations, the use of degradation and rate coefficients play an important role in the functionality of the biochemical ADM1 model. Key parameters required in ADM1 are calculated from experimental tests with the

use of specific tests. Some examples include the degradation and rate coefficients that can be acquired through the use of batch tests such as the biochemical methane potential (BMP) tests [31, 32]. The use of batch tests has been important in determining growth and decay coefficients and the BMP test is a faster, low cost method of aiding model development with drawbacks to high maintenance and development.

1.5 Research Objectives

With the lack of quantitative understandings of ammonia and acetic acid inhibition within AD modelling, these research objectives are proposed and examined in this study:

1. The primary objective was to analyse inhibition of ammonia in WAS on methane production and biogas composition given the needed but limited knowledge on ammonia inhibition on wastewater of a higher solids concentration.
2. The second objective was to analyse inhibition of acetic acid in WAS on methane production and biogas composition for a wastewater of higher solids concentration. This was done with a standalone perspective and in conjunction with the effects of ammonia inhibition on the same substrate.
3. The third objective was to model these inhibition reactions with the use of an AD model that allowed for experimental conditions to be translated to output the methane production and analysis of inhibition with the tests.

2 Methods and Analysis

2.1 Experimental Methods

The experiments were carried out using biochemical methane production (BMP) assays [31]. Using 160 mL glass bottles, lab-scale anaerobic batch reactors were operated at a mesophilic temperature of 37.5 ℃ in a shaking incubator (700L Stackable Incubated 126 Shaker, Eppendorf, USA) for a duration of 28 days with frequent biogas sampling. For this study, the batch reactors explored nine conditions with experiments varying in pH, ammonia, and acetate concentrations utilizing 50 mL of TWAS as substrate and 20 mL of inoculum with characteristics seen in Table 2.1 and Appendix B: .

Table 2.1: Characteristics of sludge used in BMP test operated at 37.5 ºC with no added toxicants for model comparison.

	Sludge I
TCOD (g/L)	38.8 ± 0.3
sCOD (g/L)	3.8 ± 0.1
TSS (g/L)	35.1 ± 1.4
VSS (g/L)	24.9 ± 0.7
TAN (g-N/L)	0.9 ± 0.1
pH	7.0 ± 0.2

The batch reactors used inoculum from a lab-scale anaerobic digester and a substrate of thickened waste activated sludge (TWAS) obtained from the Woodward Avenue Wastewater Treatment Plant in Hamilton, Ontario (Table 2.1). The inoculum digester was maintained for ten months at the same mesophilic temperature with a mean retention time of 21 days in a stand-alone incubator. The inoculum digester utilised the same substrate as the batch reactors. The TWAS was stored in a refrigerator at 4 ℃ for up

to 1 week and warmed prior to substrate utilization for the digester and batch reactors to avoid thermal shock to the inoculum. The inoculum digester and reactors were both purged with inert nitrogen gas after feed, prior to being sealed.

The nine different conditions examined with the BMP assays included three ammonia conditions and three acetate concentrations (Table 2.2). The three different ammonia values were observed with two different ammonia concentrations of 0 and 4 g-N/L and different pH conditions ranging around 7 – 9 for a neutral pH (NPH) and high pH (HPH) that is based on the amounts ammonium chloride and ammonium hydroxide added. Three acetate concentrations of 0, 20, and 40 g-COD/L (or 0, 21.3, and 42.7 g/L as acetic acid) were considered in conjunction to the three ammonia conditions with the addition of sodium acetate. These were denoted as 0VFA, 20VFA, and 40VFA, respectively. The analysis of biogas was observed for approximately 28 days with a high frequency of biogas collection occurring towards the beginning of the experiment.

Table 2.2: Experimental conditions with three varying acetate concentrations and three varying ammonia and pH concentrations with the control, 0VFA|0N.

Acetate added (as CH_3COONa) → Ammonia added ↓	0 g-COD/L **(0VFA)**	20 g-COD/L **(20VFA)**	40 g-COD/L **(40VFA)**
0 g-N/L **(0N)**	**0VFA | 0N** pH: 7.3 → 7.6	**20VFA | 0N** pH: 7.3 → 8.0	**40VFA | 0N** pH: 7.3 → 8.0
4 g-N/L as NH_4Cl **(4N-NPH)**	**0VFA | 4N-NPH** pH: 7.1 → 7.6	**20VFA | 4N-NPH** pH: 7.2 → 7.7	**40VFA | 4N-NPH** pH: 7.2 → 7.8
4 g-N/L as NH_4Cl and NH_4OH **(4N-HPH)**	**0VFA | 4N-HPH** pH: 8.9 → 7.6	**20VFA | 4N-HPH** pH: 8.8 → 7.7	**40VFA | 4N-HPH** pH: 8.9 → 7.9

2.2 Analytical Methods

The analysis was observed at the beginning and end of the 28-day BMP test and included measuring pH, conductivity (K), analysis of total solids (TS), volatile solids (VS), total suspended solids (TSS), volatile suspended solids (VSS), total chemical oxygen demand (TCOD) and soluble chemical oxygen demand (sCOD) according to the standard methods [33]. Sludge pH (SevenMulti, Mettler Toledo) was measured at the beginning and end of the experiment cycle and ranged from neutral to high pH. The suspended solids analysis used a 1.5 µm filter paper (934-AH Glass Microfiber Filters, GE Healthcare Biosciences, USA) while sCOD was measured by filtering a sample using 0.45 µm filters (28145-503 Polyethersulfone Membrane Syringe Filters with Acrylic Housing, VWR, USA) and diluting by a factor of 10.

Methane and carbon dioxide were collected as biogas and analysed with nitrogen gas using a thermal conductivity detector – gas chromatograph (TCD-GC) (SRI 8610C, SRI Instruments, USA). The TCD-GC used a molecular sieve column (ShinCarbon ST 19808, Restek, USA) and helium as the carrier gas. A nitrogen purge was conducted before and after filling the sludge components of the BMP. This purge consists of a 1 – 3-minute displacement of air with heavily concentrated nitrogen gas at a moderate flow rate. Initial analysis with the TCD-GC confirmed nitrogen was the only gas present in the first few minutes of the BMP bottle formation. During analysis, biogas volume was measured using a water displacement method with gasbags and for BMPs, the biogas volume was measured using gas-tight syringes of 5 – 50 mL capacities (50 mL, Dyna Medical Corporation, Canada).

3 Numerical Model Development and Implementation of ADM1

3.1 Kinetic Equations and Assumptions

The comprehensive AD model, ADM1, is developed by the IWA task group, and is often simplified to develop more manageable models while maintaining equivocal simulation accuracy [28]. Based on the experimental methodology of batch reactors, this mathematical model was assembled based on a non-steady state assumption and considering the objectives of this research the framework of ADM1, only the biological reactions are modelled. All 21 biological components and 19 associated reactions can be observed in Table 3.1.

Modelling the biochemical processes in ADM1 observes 21 components going through different reactions all occurring in series and parallel to each other (Figure 1.1). The disintegration of composite particulate material (X_C) involves fractionation into carbohydrates (X_{CH}), proteins (X_{PR}), lipids (X_{LI}), and inerts (X_I). The products of the hydrolysis reactions are sugars (S_{SU}), amino acids (S_{AA}), and long chain fatty acids (S_{FA}) that can be collectively observed as S_{ORG}. Fermenters (X_F) that includes sugar fermenters (X_{SU}), amino acid fermenters (X_{AA}), and long chain fatty acid beta-oxidizers (X_{FA}) rapidly convert the S_{ORG} to hydrogen gas (S_{H2}) and volatile fatty acids S_{VFA}, represented in ADM1 by butyrate (S_{BU}), valerate (S_{VA}), propionate (S_{PRO}), and acetate (S_{AC}) in the acidogenesis step. Methanogenesis is completed with S_{VFA} and S_{H2} being converted into methane (S_{CH4}) by volatile fatty acid degraders (X_{VFA}), collectively valerate and butyrate beta-oxidizers (X_{C4}), propionate beta-oxidizers (X_{PRO}) and acetoclastic methanogens (X_{AC}) and hydrogenotrophic methanogens (X_{H2}).

The Monod equation was developed based on Michalis-Menten enzyme kinetic equations and have been used to describe specific biological processes based on the Monod model, including Haldane, Yano, Aiba, and Edwards models. The reactions used in this model are mostly composed with Monod-type kinetic equations with the exception of Haldane kinetics used in the acetate uptake reaction (Table 3.1).

Assumed linear changes in pH and ammonia have also been implemented in the model to account for the change in the kinetic and inhibition equations for the 28-day duration. The initial values developed for the composition of TWAS (Table 3.2) were obtained from previous studies that analysed the use of similar substrate with adjustments for temperature [36, 37]. Kinetic coefficients were slightly altered from the original ADM1 model with minor adjustments to temperature for a mesophilic temperature of 37.5 ºC while some fractions listed were altered for better representation of hydrogenic methanogenesis contribution to methane production (Table 3.3).

Table 3.1: Kinetic rate expressions used in the mathematical model. A rate expression can be obtained: $R_{i=}\sum_{i,j=1}^{j=19} r_{i,j} * Rate_{i,j}$

	Component (i) →	1	2	3	4	5	6	7	8	9	**Rate (g-COD L^{-1} d^{-1})**
j	**Process**	S_{SU}	S_{AA}	S_{FA}	S_{VA}	S_{BU}	S_{PRO}	S_{AC}	S_{H2}	S_{CH4}	
1	Disintegration										$k_{dis}X_C$
2	Hydrolysis of carbohydrates	1									$k_{hydch}X_{CH}$
3	Hydrolysis of proteins		1								$k_{hydpr}X_{PR}$
4	Hydrolysis of lipids	1- $f_{fa,li}$		$f_{fa,li}$							$k_{hydli}X_{LI}$
5*	Uptake of sugars	-1				$(1-Y_{su})f_{bu,su}$	$(1-Y_{su})f_{pro,su}$	$(1-Y_{su})f_{ac,su}$	$(1-Y_{su})f_{h2,su}$		$k_{su}\frac{S_{SU}}{K_{ssu}+S_{SU}}X_{SU}I_1$
6*	Uptake of amino acids		-1		$(1-Y_{aa})f_{va,aa}$	$(1-Y_{aa})f_{bu,aa}$	$(1-Y_{aa})f_{pro,aa}$	$(1-Y_{aa})f_{ac,aa}$	$(1-Y_{aa})f_{h2,aa}$		$k_{aa}\frac{S_{AA}}{K_{saa}+S_{AA}}X_{AA}I_1$
7	Uptake of LCFA			-1				$(1-Y_{fa})0.7$	$(1-Y_{fa})0.3$		$k_{fa}\frac{S_{FA}}{K_{sfa}+S_{FA}}X_{FA}I_2$
8	Uptake of valerate				-1		$(1-Y_{c4})0.54$	$(1-Y_{c4})0.31$	$(1-Y_{c4})0.15$		$k_{c4}\frac{S_{VA}}{K_{sc4}+S_{VA}}X_{C4}\frac{1}{1+S_{BU}/S_{VA}}I_2$
9	Uptake of butyrate					-1		$(1-Y_{c4})0.8$	$(1-Y_{c4})0.2$		$k_{c4}\frac{S_{BU}}{K_{sc4}+S_{BU}}X_{C4}\frac{1}{1+S_{VA}/S_{BU}}I_2$
10	Uptake of propionate						-1	$(1-Y_{pro})0.57$	$(1-Y_{pro})0.43$		$k_{pro}\frac{S_{PRO(1)}}{K_{spro}+S_{PRO(1)}}X_{PRO}I_2$
11’	Uptake of acetate							-1		$(1-Y_{ac})$	$k_{ac}\frac{S_{AC}}{K_{sac}+S_{AC}}X_{AC}I_3'$
12’	Uptake of hydrogen								-1	$(1-Y_{h2})$	$k_{h2}\frac{S_{H2}}{K_{sh2}+S_{H2}}X_{H2}I_1'$
13	Decay of X_{su}										$k_{decxsu}X_{SU}$
14	Decay of X_{aa}										$k_{decxaa}X_{AA}$
15	Decay of X_{fa}										$k_{decxfa}X_{FA}$
16	Decay of X_{c4}										$k_{decxc4}X_{C4}$
17	Decay of X_{pro}										$k_{decxpro}X_{PRO}$
18	Decay of X_{ac}										$k_{decxac}X_{AC}$
19	Decay of X_{h2}										$k_{decxh2}X_{H2}$

	Component (i) →	11	12	13	14	15	16	17	18	19	20	21	**Rate (g-COD L^{-1} d^{-1})**
j	**Process**	X_C	X_{CH}	X_{PR}	X_{LI}	X_{SU}	X_{AA}	X_{C4}	X_{PRO}	X_{AC}	X_{H2}	X_I	
1	Disintegration	-1											$k_{dis}X_C$
2	Hydrolysis of carbohydrates		-1										$k_{hydch}X_{CH}$
3	Hydrolysis of proteins			-1									$k_{hydpr}X_{PR}$
4	Hydrolysis of lipids				-1								$k_{hydli}X_{LI}$
5	Uptake of sugars					Y_{su}							$k_{su}\frac{S_{SU}}{K_{ssu}+S_{SU}}X_{SU}I_1$
6	Uptake of amino acids						Y_{aa}						$k_{aa}\frac{S_{AA}}{K_{saa}+S_{AA}}X_{AA}I_1$
7	Uptake of LCFA							Y_{fa}					$k_{fa}\frac{S_{FA}}{K_{sfa}+S_{FA}}X_{FA}I_2$
8	Uptake of valerate								Y_{c4}				$k_{c4}\frac{S_{VA}}{K_{sc4}+S_{VA}}X_{C4}\frac{1}{1+S_{BU}/S_{VA}}I_2$
9	Uptake of butyrate								Y_{c4}				$k_{c4}\frac{S_{BU}}{K_{sc4}+S_{BU}}X_{C4}\frac{1}{1+S_{VA}/S_{BU}}I_2$
10	Uptake of propionate									Y_{pro}			$k_{pro}\frac{S_{PRO(1)}}{K_{spro}+S_{PRO(1)}}X_{PRO}I_2$
11’	Uptake of acetate										Y_{ac}		$k_{ac}\frac{S_{AC}}{K_{sac}+S_{AC}}X_{AC}I'_3$
12’	Uptake of hydrogen											Y_{h2}	$k_{h2}\frac{S_{H2}}{K_{sh2}+S_{H2}}X_{H2}I'_1$
13	Decay of X_{su}	1				-1							$k_{decxsu}X_{SU}$
14	Decay of X_{aa}	1					-1						$k_{decxaa}X_{AA}$
15	Decay of X_{fa}	1						-1					$k_{decxfa}X_{FA}$
16	Decay of X_{c4}	1							-1				$k_{decxc4}X_{C4}$
17	Decay of X_{pro}	1								-1			$k_{decxpro}X_{PRO}$
18	Decay of X_{ac}	1									-1		$k_{decxac}X_{AC}$
19	Decay of X_{h2}	1										-1	$k_{decxh2}X_{H2}$

* Modifications to fractions as seen in Table 3.3

‘ Inhibition terms and rate equations outlined in Table 3.4

Fully derived equations can be found in Appendix A; Equations shown were reproduced using the equations presented in ADM1 [28].

$$I_1 = I_{ph}I_{IN,lim}$$
$$I_2 = I_{ph}I_{IN,lim}I_{h2,x}$$
$$I'_3 = I_{ph}I_{IN,lim}I_{NH,Xac}I_{HAC,Xac}$$
$$I'_1 = I_{ph}I_{IN,lim}I_{NH3,Xh2}I_{HAC,Xh2}$$

Table 3.2: Initial composition of sludge, used as initial conditions for ADM1 simulations.

Model parameter	Symbol	Sludge I[a] (g-COD L^{-1})
Composites	X_C	1.1×10^{0}
Particulate Inerts	X_I	9.9×10^{0}
Carbohydrates	X_{CH}	2.7×10^{0}
Proteins	X_{PR}	1.1×10^{1}
Lipids	X_{LI}	2.7×10^{0}
Sugar fermenters	X_{SU}	2.6×10^{0}
Amino acid fermenters	X_{AA}	2.6×10^{0}
Long-chain fatty acid beta-oxidizers	X_{FA}	2.2×10^{0}
Valerate and butyrate beta-oxidizers	X_{C4}	7.3×10^{-3}
Propionate beta-oxidizers	X_{PRO}	4.4×10^{-3}
Acetoclastic methanogens	X_{AC}	1.0×10^{-2}
Hydrogenotrophic methanogens	X_{H2}	7.3×10^{-1}
Sugars	S_{SU}	1.8×10^{0}
Amino acids	S_{AA}	7.4×10^{-1}
Long-chain fatty acids	S_{FA}	1.8×10^{-5}
Valerate	S_{VA}	2.6×10^{-2}
Butyrate	S_{BU}	2.6×10^{-2}
Propionate	S_{PRO}	2.6×10^{-2}
Acetate	S_{AC}	2.6×10^{-2}
Hydrogen gas	S_{H2}	5.3×10^{-9}
Methane gas	S_{CH4}	0

[a] Sludge I values were calculated based on comparison of measured sludge from [36] and experimental data (Table 2.1). These values are used as the initial conditions of the model.

Table 3.3: Kinetic parameters, rates and stoichiometric coefficients used in mathematical model for a temperature of 37.5 ºC. Equations in Appendix A.

Model parameter	Symbol	Value	Unit
First order decay rate of degraders, beta-oxidizers, methanogens	k_{dec}	2.2×10^{-2}	d^{-1}
First order composite disintegration rate	k_{dis}	5.4×10^{-1}	d^{-1}
First order hydrolysis rate	k_{hyd}	1.0×10^{1}	d^{-1}
Monod Max. specific sugar utilization rate	k_{su}	3.1×10^{1}	d^{-1}
Monod Max. specific amino acid utilization rate	k_{aa}	5.2×10^{1}	d^{-1}
Monod Max. specific long-chain fatty acid utilization rate	k_{fa}	6.4×10^{0}	d^{-1}
Monod Max. specific valerate and butyrate utilization rate	k_{c4}	2.1×10^{1}	d^{-1}
Monod Max. specific propionate utilization rate	k_{pro}	1.4×10^{1}	d^{-1}
Monod Max. specific acetoclastic methanogenesis rate	k_{ac}	9.1×10^{0}	d^{-1}
Monod Max. specific hydrogenotrophic methanogenesis rate	k_{h2}	3.1×10^{1}	d^{-1}
Half-saturation value for sugar utilization	$K_{S,su}$	5.4×10^{-1}	g-COD L^{-1}
Half-saturation value for utilization	$K_{S,aa}$	3.0×10^{-1}	g-COD L^{-1}
Half-saturation value for utilization	$K_{S,fa}$	4.0×10^{-1}	g-COD L^{-1}
Half-saturation value for utilization	$K_{S,c4}$	2.2×10^{-1}	g-COD L^{-1}
Half-saturation value for utilization	$K_{S,pro}$	1.1×10^{-1}	g-COD L^{-1}
Half-saturation value for utilization	$K_{S,ac}$	1.6×10^{-1}	g-COD L^{-1}
Half-saturation value for utilization	$K_{S,h2}$	8.9×10^{-6}	g-COD L^{-1}
Yield of fermenters on sugar	Y_{su}	1.0×10^{-1}	g-COD g-COD^{-1}
Yield of fermenters on amino acids	Y_{aa}	8.0×10^{-2}	g-COD g-COD^{-1}
Yield of beta-oxidizers on long-chain fatty acids	Y_{fa}	6.0×10^{-2}	g-COD g-COD^{-1}
Yield of beta-oxidizers on valerate and butyrate	Y_{c4}	6.0×10^{-2}	g-COD g-COD^{-1}
Yield of beta-oxidizers on propionate	Y_{pro}	4.0×10^{-2}	g-COD g-COD^{-1}
Yield of acetoclastic methanogens on acetic acid	Y_{ac}	5.0×10^{-2}	g-COD g-COD^{-1}
Yield of hydrogenotrophic methanogens on hydrogen	Y_{h2}	6.0×10^{-2}	g-COD g-COD^{-1}
Fraction of soluble inerts from composites	$f_{si,xc}$	1.0×10^{-2}	-
Fraction of particulate inerts from composites	$f_{xi,xc}$	2.5×10^{-1}	-
Fraction of carbohydrates from composites	$f_{ch,xc}$	2.0×10^{-1}	-
Fraction of proteins from composites	$f_{pr,xc}$	2.0×10^{-1}	-
Fraction of lipids from composites	$f_{li,xc}$	2.5×10^{-1}	-
Fraction of fatty acids from lipids	$f_{fa,li}$	9.5×10^{-1}	-
Fraction of hydrogen from sugars*	$f_{h2,su}$	3.8×10^{-1}	-
Fraction of butyrate from sugars	$f_{bu,su}$	1.3×10^{-1}	-
Fraction of propionate from sugars	$f_{pro,su}$	2.7×10^{-1}	-
Fraction of acetate from sugars*	$f_{ac,su}$	2.2×10^{-1}	-
Fraction of hydrogen from amino acids*	$f_{h2,aa}$	1.2×10^{-1}	-
Fraction of valerate from amino acids*	$f_{va,aa}$	2.6×10^{-1}	-
Fraction of butyrate from amino acids	$f_{bu,aa}$	5.0×10^{-2}	-
Fraction of propionate from amino acids	$f_{pro,aa}$	2.1×10^{-1}	-
Fraction of acetate from amino acids*	$f_{ac,aa}$	3.6×10^{-1}	-

Parameter values are suggested from ADM1 [28] with temperature-adjusted values calculated based on Arrhenius values derived from suggested values at 35 ºC and 55 ºC

* Values altered and used in model (increase for hydrogen fractions, remained the same for butyrate and propionate fractions, decreased for acetate and valerate fractions)

3.2 Inhibition Equations

The main inhibition terms in ADM1 focus on inorganic-nitrogen, pH, hydrogen, and ammonia inhibitions. Inorganic-nitrogen inhibition in AD is a value that increases from 0 – 1 with increased concentration with an inhibition parameter of 10^{-4} M for the purpose of having a sufficient concentration of nitrogen for necessary biological processes ($r_5 – r_{12}$). The empirical pH inhibition function is based on pH boundary parameters particular for each process (Table 3.4): fermentation and anaerobic oxidation ($r_5 – r_{10}$), acetoclastic methanogenesis (r_{11}), and hydrogenotrophic methanogenesis (r_{12}). One specified issue with this pH function is its lack of inhibition effecting higher pH conditions. Hydrogen inhibition on anaerobic oxidation processes ($r_7 – r_{11}$) also takes into account the amount of hydrogen and an inhibition parameter in a simple inhibition equation (Table 3.4). Ammonia inhibition in the generic ADM1 model looks at inhibition with the FAN concentration implemented in a simple inhibition equation. These inhibition terms have certain limitations on the assumptions and thus, a further look and implementation of inhibition terms for certain concentrations is also introduced.

The generic ADM1 ammonia inhibition term observes at inhibition based on FAN but not the ammonium toxicity. It was reported that FAN and ammonium inhibition need to be jointly determined and a threshold inhibition function can describe this inhibition with the advantage of identifying lower and upper inhibition limits at which the concentration starts, completes and also identifies the inhibition concentration at 50% inhibited (Table 3.4) [19]. The pH, TAN, and solids concentrations used in the development of the inhibition function are akin to the values used in this experimental

study. In implementing the inhibition term, negative impacts only occurred on acetoclastic methanogens, and while these microorganisms are more affected, hydrogenotrophic methanogens would need to be inhibited for the expected lack of methane production. This effect of ammonia on hydrogenotrophic methanogens was imposed in the model with a simple inhibition equation with FAN as the main factor of inhibition (Table 3.4).

The original ADM1 does not define any acetic acid inhibition, however, this known inhibition factor has been implemented in previous studies through a variety of methods. Some of these methods include the use of a simple inhibition equation focused on acetate, VFAs, and/or SCFAs with a focus on the effect of substrate inhibition by acetate. Haldane kinetics aids in posing an inhibition within the growth term as a function of the substrate to induce an inhibitory effect on the substrate (Table 3.4). Unlike non-competitive inhibition terms, Haldane is an un-competitive inhibition term that is frequently chosen to represent the methanogenesis reaction due to its use for describing a wide range of initial acetate concentrations [34, 35]. Having been used to account for the inhibition of acetoclastic methanogenesis by high acetate concentrations, it produces a similar sigmoidal methane accumulation and acetate depletion curves to that of Monod. As was evaluated for ammonia inhibition, the effect of acetic acid inhibition in the production of methane occurs for both acetate and acetic acid, thus both were used with the inhibition caused by acetic acid having less of an effect and implemented with a simple inhibition equation (Table 3.4). Hydrogenotrophic methanogens were also expected to be inhibited due to accumulation and this was implemented with a simple inhibition equation for acetic acid (Table 3.4).

Table 3.4: Inhibition equations and terms.

Type	Equation	Additional information	Ref
pH Inhibition (Empirical Function)	$I_{\substack{PHn \\ (1,2,3)}} = \begin{pmatrix} e^{\left[-3*\left(\frac{ph-ph_{ul,n}}{ph_{ul,n}-ph_{ll,n}}\right)^2\right]}, & if\ ph \le ph_{ul,n} \\ 1, & if\ ph > ph_{ul,n} \end{pmatrix}$	pH_{LL}, pH_{UL} • For $r_5 – r_{10}$ (I_{PH1}) = 4, 5.5 • For r_{11} (I_{PH2}) = 6, 7 • For r_{12} (I_{PH3}) = 5, 6	[28]
Inorganic Nitrogen (Simple Inhibition)	$I_{IN,lim} = \frac{1}{1 + K_{SIN}/S_{IN}}$		[28]
Hydrogen inhibition on anaerobic oxidation (Simple Inhibition)	$I_{h2,x} = \frac{1}{1 + S_{H2}/K_{IH2,x}}$	Applies to LCFA, butyrate, valerate, propionate	[28]
Free ammonia & ammonium inhibition on X_{AC}, acetoclastic methanogens (Threshold Inhibition)	$I_{NH,XAC} = I_{NH3} I_{NH4+}$ $I_{NHx} = \begin{cases} 1, & S_i \le K_{i,min} \\ e^{-2.77259\left(\frac{S_i - K_{Imin}}{K_{Imax} - K_{Imin}}\right)^2}, & S_i > K_{i,min} \end{cases}$	K_{Imin} and K_{Imax} determined individually for NH_3 and NH_4 (Table 4.1)	[19]
Free ammonia inhibition on X_{H2}, hydrogenotrophic methanogens, (Simple Inhibition)	$I_{NH3,Xh2} = \frac{1}{1 + S_{NH3}/K_{INH3,Xh2}}$	$K_{INH3,Xh2}$ (Table 4.1)	
Acetate inhibition on X_{AC}, acetoclastic methanogens (Haldane Inhibition)	$r'_{11} = k_{ac} \frac{S_{AC}}{K_{sac} + S_{AC} + S_{AC}^2/K_{IAC,Xac}} X_{AC} I_1$	$K_{IAC,Xac}$ (Table 4.2)	
Acetic acid inhibition on X_{AC}, acetoclastic methanogens (Simple Inhibition)	$I_{HAC,Xac} = \frac{1}{1 + S_{HAC}/K_{IHAC,Xac}}$	$K_{IHAC,Xac}$ (Table 4.2)	
Acetic acid inhibition on X_{H2}, hydrogenotrophic methanogens (Simple Inhibition)	$I_{HAC,Xh2} = \frac{1}{1 + S_{HAC}/K_{IHAC,Xh2}}$	$K_{IHAC,Xh2}$ (Table 4.2)	

3.3 Numerical Solution Method

Algebraic equations, defining all individual components, were converted from differential equations in ADM1 using the finite difference method and solved implicitly using fixed-point iterations with a relative error convergence criterion of 10^{-3}. A 10-minute time-step was used to simulate the model throughout the 28-day experimental duration. These equations can be observed in Appendix A. This model has been implemented using visual basic application (VBA).

4 Results and Discussions

4.1 Analysis of Hydrolysis on Ammonia Concentrations for Inhibitions

The primary observations for the effects of ammonia inhibition focused on the variation between the no added acetate (0VFA) conditions with the 0 g-N/L condition (0N) and the 4 g-N/L at the neutral pH condition (4N-NPH) to solely observe the effect of increased inhibition with increased ammonia concentration. The amount of ammonia released is seen in the difference between the initial and final ammonia values (Figure 4.1), occurring through the hydrolysis of amino acids. Both 0N and 4N-NPH conditions released similar amounts of ammonia, proving that the concentration of ammonia did not affect hydrolysis in AD. The pH increased with these conditions as the hydrolysis of amino acids incurred a rise in alkalinity (Table 2.2). The increase in TAN and pH corresponded to the increase in FAN for both conditions from the start to the end of the experiment but TAN was the bigger factor that contributed to the higher FAN present at the end of the 4N-NPH condition compared to the 0N condition.

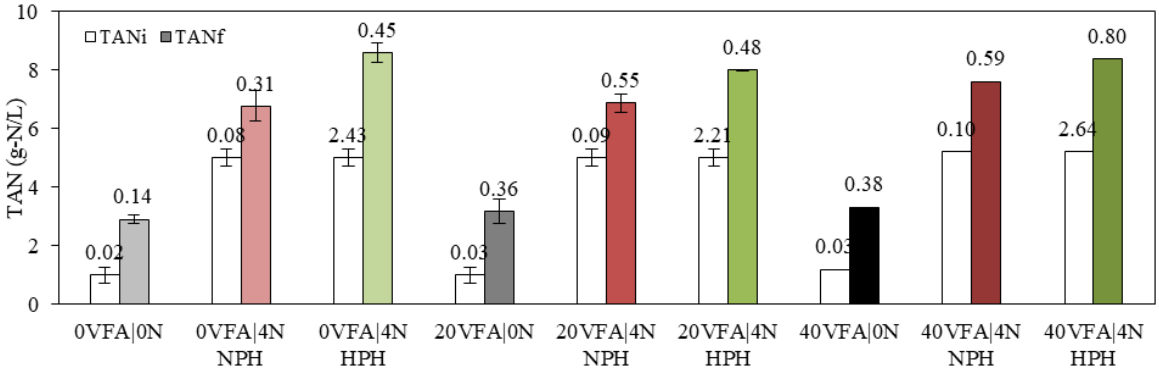

Figure 4.1: Ammonia concentrations ascertained at the beginning and end of BMP with 28-day duration graphed with labeled FAN (as g-N/L) values calculated based on corresponding TAN and pH values (Table 2.2) in accordance to Eq. (1.2).

The secondary observations for the effects of ammonia inhibition examined the effect of pH on ammonia inhibition, by analysing the variations of the 4 g-N/L (4N) conditions with the neutral and high pH conditions exclusively. Observation of the ammonia released at the 0VFA condition (Figure 4.1) indicated that about double the amount of ammonia was released with 1.8 g-N/L for 4N-NPH compared to 3.6 g-N/L for 4N-HPH. This increase for the 4N-HPH condition implied hydrolysis of ammonia and the larger effect of inhibition; preventing uptake of organic nitrogen for subsequent processes. Dependent on the methane production and utilization of total and soluble COD, this distinction could be better analysed. FAN was more dominant than ammonium at higher pH concentrations and had more inhibitory effects. Thus, 4N-HPH was suggested to be more inhibitory with higher FAN concentrations initially while the drop in pH encouraged the effect of reactive toxicity with a readjustment to toxicity effects.

Recognizing the effects of ammonia and pH with the 0 g-CODL (0VFA) acetate condition, inhibition at 4N-NPH and 4N-HPH conditions are the next observations with 20 g-COD/L (20VFA) and 40 g-COD/L (40VFA). Similar amounts of TAN were released and average FAN concentrations were observed at the 0N and 4N-NPH conditions observing similar solubilization (Figure 4.1). Average FAN concentrations increased from 0.08, 0.19, to 0.21 g-N/L for 0N and 0.2, 0.32, to 0.34 g-N/L for 4N-NPH with increased acetate concentrations. The similarities for 20VFA and 40VFA at both these neutral pH conditions indicated the presence of comparable inhibitions that focused on the ammonia and pH concentrations. Ammonia released for 4N-HPH conditions at 20VFA and 40VFA was similar for their 4N-NPH counterparts, indicative of similar solubilization and suspected

uptake of organic nitrogen inhibitions that could have been aided by any acetate addition. Observing pH for these higher acetate conditions did not suggest that a decrease in pH was found with increased acetate addition (Table 2.2) and the FAN concentrations for these conditions still suggested a level of inhibition that increased with acetate addition at a higher pH. High TAN concentration was the main source of free ammonia to the inhibition mechanism but the contribution of pH towards increased FAN concentrations was also a highly influential factor. With analysis of TAN, the pH and FAN were larger factors for ammonia inhibition than acetic acid inhibition.

4.2 Effect of Ammonia Inhibition on Methane Production

Methane production demonstrated an observable effect of the efficiency of the AD process. The effects of ammonia inhibition were particularly observable in the difference between the amount of methane produced by the 0 g-N/L (0N) test with a higher yield of methane production compared to both of the 4 g-N/L (4N) tests with the no acetate (0VFA) condition (Figure 4.2a). The 0N condition observed a steady production of methane with an initial rate of about 2 g-COD/L/d while the 4N-NPH exhibited inhibition effects with a slight lag phase of about 2-3 days and a decreased rate over another 15-18 days, until the methane production started to decrease to a rate change of about 1 g-COD/L/d. Both methane production curves appeared to reach similar methane production rates towards the end of the test, however, the added ammonia condition achieved about 22% less efficiency with biogas production. Consistent with the observations of FAN, inhibition was evident in methane production curves suggesting the 4N-NPH test had more ammonia inhibition than the 0VFA|0N test.

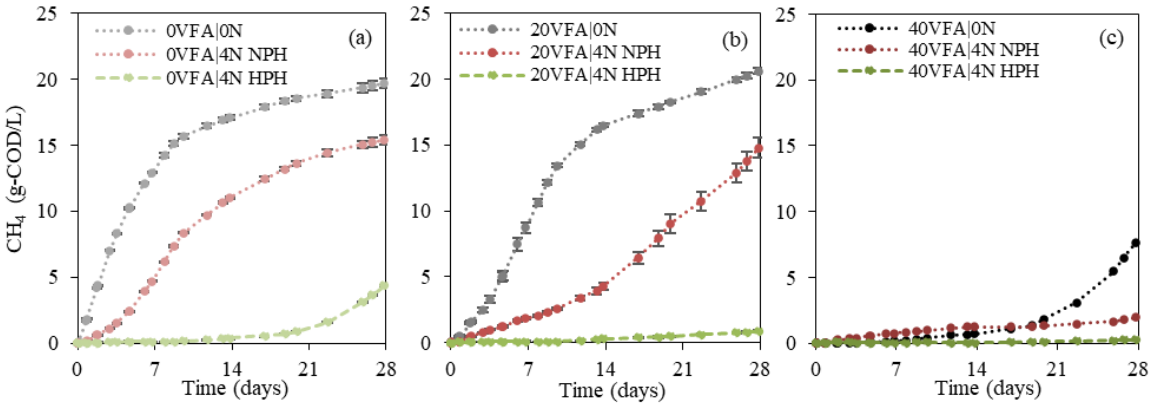

Figure 4.2: Methane production from BMP experimental tests for: (a) 0VFA conditions, (b) 20VFA conditions, and (c) 40VFA conditions. Volumetric methane curves normalized with initial COD are shown in Figure B.1.

Evaluating the second observations, the 4N-NPH test had a higher yield of methane production in comparison to the 4N-HPH test (Figure 4.2a). At the NPH condition, the lag phase was a mere 2- to 3-day duration followed by a decreased rate of methane production. Meanwhile the 4N-HPH methane production observed a lag phase of 20 days followed by approximately the same rate of methane. FAN inhibition mechanisms affecting methanogenesis included the hydrophobicity of FAN enabling intracellular accumulation until gradual reduction of pH decreased this toxicity, producing methane after a lag phase with the 4N-HPH test. With the NPH test, FAN concentrations increased, attributing to the decreased rate of methane production evident in the methane production curve when compared to the 0N test (Figure 4.2a). In comparison to the 0N test, the 4N-NPH and 4N-HPH tests had a 22% and 78% decrease in biogas production, average pH values of 7.35 and 8.25, and average FAN concentrations of 0.2 g-N/L and 1.44 g-N/L, respectively. Thus, increased FAN and increased change in TAN caused the decreased yield of methane through ammonia inhibition.

4.3 Combined Effect of Acetic Acid Inhibition and Ammonia Inhibition on Methane Production

The addition of acetate was used to observe the behaviour of acetic acid inhibition specifically to total VFA inhibition as it directly impacted the acetoclastic methanogenesis pathway towards methane production. The experimental conditions focused on the variation of the concentrations of acetate at 0 g-CODL (0VFA), 20 g-COD/L (20VFA), and 40 g-COD/L (40VFA) specifically at the 0 g-N/L (0N) condition to explicitly observe this acetic acid inhibition and then at the 4 g-N/L neutral pH (4N-NPH) condition to observe the added effect of ammonia inhibition with all of the methane production graphs in Figure 4.2. The 0VFA|0N test observed a steady production of methane until a change in slope occurred around day 7 and produced about 15 g-COD/L of methane while the 20VFA|0N condition observed a slower rate of methane production for the first 3-4 days, and increased thereafter to produce about 10 g-COD/L of methane. Unlike the observed effects for ammonia inhibition, an induced lag phase was not as apparent for the 20VFA condition but a decrease in methane production rate was observed. The 40VFA condition was the most inhibited of the 0N acetate conditions and suggested an initial lag phase for 10 days followed by a recovery of methanogenesis during which the rate of methane production kept increasing. The average rate for 40VFA|0N was almost equal to that of the previous two observed. Final methane yields changed in 5% increase and 61% decrease, in comparison to the 0VFA|0N test, for these acetate conditions. The rate observed at the end of these conditions indicates that the maximum methane potential for the 20VFA condition had not been met and the increased organic concentrations had improved methane production but organic overload caused more severe inhibitory effects on the 40VFA

condition. This is consistent with other studies observing the effect of acetate concentrations below and above 10 g-COD/L [25, 38]. The overall inhibition trend noted that the increased acetate concentrations of sodium acetate inhibited the AD process.

Methane production with the increased acetate conditions for the 4N-NPH condition showed few differences in analyses compared to the 0N conditions as is evident in Figure 4.2. Firstly, the similarities between 0VFA and 20VFA conditions resulted in remarkably similar final methane yields at the end of the experiment for both at the 0N and 4N-NPH conditions. As speculated, the 20VFA conditions with increased organic concentrations had improved methane production as demonstrated with the final rates of methane production. At 4N-NPH, a brief lag phase occurred for the 0VFA condition while methane production rates decreased for 20VFA and 40VFA. After steadily increasing over the first 14 days, the rate of methane production increased for the 20VFA condition and was negligible for the 40VFA condition. Comparison of the percent decrease at 4N-NPH to the 0VFA test was 25% and 90% for 20VFA and 40VFA, respectively. The influence on the lag phase and rate of methanogenesis indicated acetic acid inhibition throughout the process for the 4N-NPH condition. At 4N-HPH, little methane production was observed at 0VFA while negligible amounts were observed for the increased acetate conditions (Figure 4.2). For all COD conditions, 4N-HPH exhibited longer lag phases with little or no methane production at the same rate or decreased rate with the percent decrease to the 0VFA|0N test was 96% and 99% for the high pH tests of 20VFA and 40VFA, respectively. The only 4N-HPH condition to produce a decent amount of methane was the 0VFA condition, thus the

combined inhibition effect of ammonia addition with increased acetate conditions (20VFA and 40VFA) was more severe in comparison.

4.4 Inhibition Effects on VSS Reduction

VSS reduction was used determine the efficacy of the AD process by way of the reduction of volatile solids, focusing on the degree of hydrolysis and solubilization. Primary observations of VSS reduction (Figure 4.3a) was focused on the first group of 0VFA conditions outlining the lack of difference in ammonia concentrations from no ammonia (0N) to 4 g-N/L of ammonia (4N) at the neutral and high pH conditions (NPH and HPH). VSS was expected to decrease for lower methane yields due to increased inhibition present with 4N conditions. The same amount of reduction occurred for all 0VFA conditions, emphasizing that the same extent of hydrolysis was reached. Further observations looked to the 0N conditions with increased acetate conditions from 0, 20, to 40 g-COD/L (0VFA, 20VFA, 40VFA) and observed a decrease for the highest acetate condition. VSS reduction was lower at the 40VFA condition, exemplifying the lack of organic-solids reduction for the increased acetate condition by acetic acid inhibition on hydrolysis. Further analysis at both 4N conditions observed that less reduction is also present at the 20VFA condition but still greatly decreased with the 40VFA condition. VSS reduction was more seriously affected with increased acetate conditions, determining that inhibition occurred within acetogenesis and influenced methanogenesis.

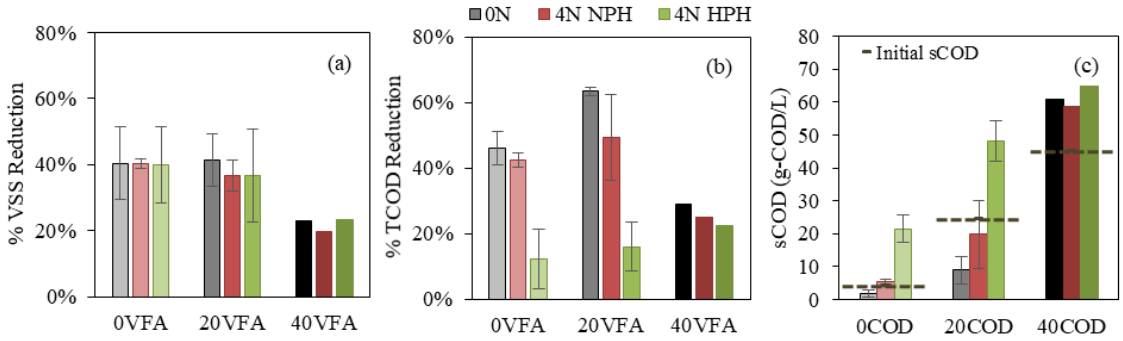

Figure 4.3: Solids analysis from the initial and final points of the BMP experimental tests showing: (a) VSS percent reduction, (b) TCOD percent reduction, and (c) final sCOD with initial sCOD values of 4.2, 24.2, and 44.8 g-COD/L for 0VFA, 20VFA, and 40VFA, respectively.

4.5 Inhibition Effects on Total and Soluble COD

The production of methane was the removal mechanism that attributed to a reduction in the measurable chemical oxygen demand in AD and it could be noticed that the methane curves directly correspond to the total chemical oxygen demand (TCOD) reduction based on this idea. The conditions that showed detrimental effects with methane production had a smaller reduction of TCOD regardless of initial conditions (Figure 4.2a and Figure 4.3b). For the 0 g-COD/L (0VFA) condition, the difference in the TCOD reduction with 0 g-N/L (0N) and 4 g-N/L neutral pH (4N-NPH) was minimal at 45% and 40%, respectively. This made the TCOD reduction values for 4N-NPH and for 4N-HPH about 88% and 22% of the 0N test, respectively. These values were almost identical to the reduction in methane production (Figure 4.3b). For the secondary observations, the 40 g-COD/L (40VFA|0N) condition showed similar trends to the 0VFA|0N test with a methane reduction and TCOD reduction value at 50%. However, the 20 g-COD/L (20VFA|0N) condition observed a greater TCOD reduction compared to the 0VFA|0N test but was about equal in final methane yield. The increase in TCOD reduction for the 20VFA condition

was also evident for the 4N-NPH and 4N-HPH conditions and might have been a representative of a benefit of the increased acetate as TWAS is not known to contain high amounts of organic content. The trend within the 20VFA and 40VFA sets decreased at increased FAN, as expected. While the 40VFA was consistent in the trend with decreased methane production, the degree of decreased TCOD was not as proportional to the other COD conditions, possibly due to the lack of methanogenesis overall with increased acetate. However, due to the lack of a duplicate value for this acetate condition, it was not possible to determine the extent of the error in this measurement nor the extent of inhibition evaluated with any other graphs. Overall, TCOD reduction correlated proportionally for methane production, with more distinctive amounts for the less inhibited conditions.

The soluble chemical oxygen demand (sCOD) had similarities to TCOD where the reduction as influenced by the uptake by methanogenic microorganisms. Within the 0VFA condition, the final sCOD was low compared to the initial measurement for the 0VFA|0N test but there was a slight increase in initial to final sCOD for the 4N-NPH test and a much larger increase for the 4N-HPH test (Figure 4.3c). This finding indicated consistency with TCOD reduction and production of methane as the hydrolysis reactions occurred, but the inhibition effects on methanogenesis prevented the use of the soluble organic matter for subsequent subprocesses for the 4N-NPH and 4N-HPH tests to different levels. The substantial increase for the 4N-HPH condition could have been related to the influence of the TAN released for this condition as the inhibition prevented uptake of soluble organic nitrogen for methanogenesis where the difference between 4N-NPH and 4N-HPH for sCOD percent increase was about 8 times greater for 4N-HPH and TAN release was about

2 times greater for 4N-HPH. Initial sCOD values increased from the 0VFA condition by approximately 20 and 40 g-COD/L through the addition of sodium acetate for the 20VFA and 40VFA conditions. Further observations noticed the reduction for 0N conditions with 0VFA and 20VFA, but an increase for 40VFA. The increase for all the 40VFA conditions observed the acetic acid inhibition influence on sCOD uptake, justified by the corresponding decreased methane production curves (Figure 4.2c). For the remaining 20VFA conditions, only the 4N-NPH condition had sCOD reduction while the 4N-HPH had an increase similar to that of the 0VFA condition and both were justified by the increased methane production curves (Figure 4.2b). Thus, observations of the sCOD decrease correspond to the conditions with increased methane production curves while those exhibiting inhibition (by ammonia, specifically) have a correlation to the amount of organic nitrogen.

4.6 Model Validation

The model development was validated through a comparison to that of Hirmiz et al. and used identical influent characterization [36]. S_{ORG}, S_{VFA}, S_{CH4}, X_{H2}, X_{VFA}, X_F, S_I, and X_I were compared between the developed model simulations and previously reported results. Overall, verification of the model was confirmed (Figure 4.4).

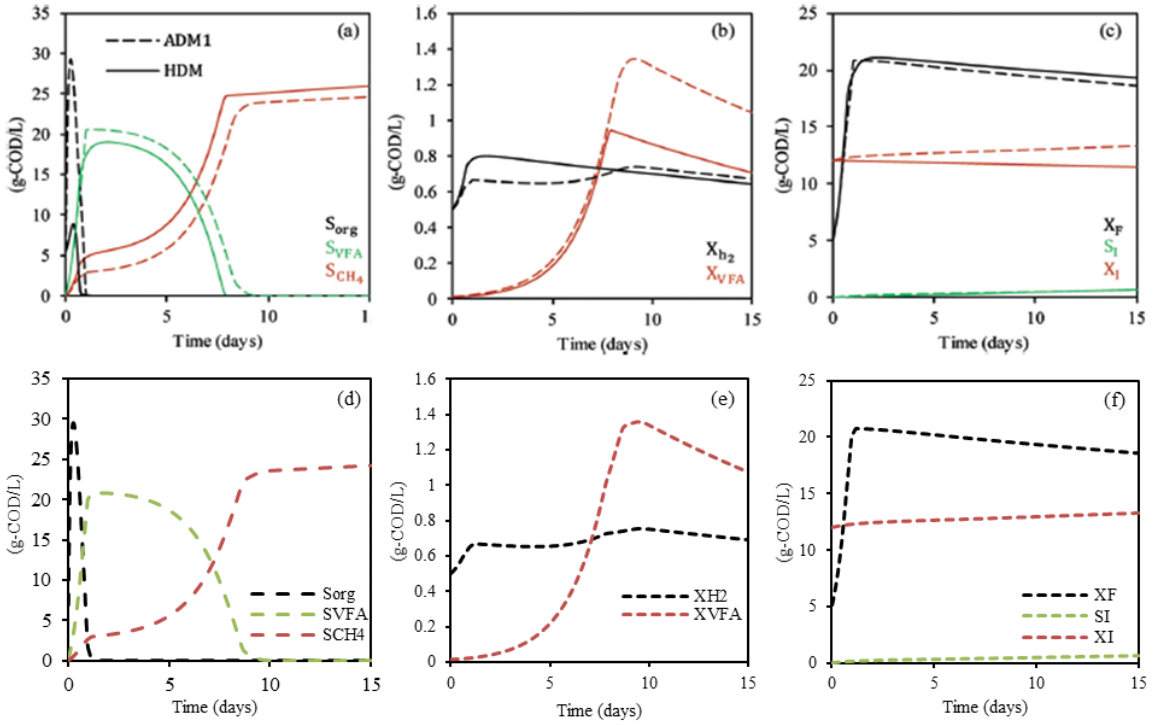

Figure 4.4: Comparison of simulation results between the ADM1 simulation (dashed line) from the model in Hirmiz et al. [36] (a, b, c) and current model (d, e, f). Simulation results include: (a, d) methane gas, volatile fatty acids, and soluble organic monomer; (b, e) volatile fatty acid degraders and hydrogenotrophic methanogens; (c, f) fermenters, inert suspended solids, and soluble inerts. Simulations were run for 15 days.

4.7 Model Simulations for Ammonia Inhibition

The implementation of ammonia inhibition in this model was based on the threshold inhibition function in Eq. (4.1), utilizing Eq. (4.2) for both ammonia components:

$$I_{NH,XAC} = I_{NH3} I_{NH4+} \tag{4.1}$$

$$I_{NHx} = \begin{cases} 1, & S_i \leq K_{i,min} \\ e^{-2.77259\left(\frac{S_i - K_{Imin}}{K_{Imax} - K_{Imin}}\right)^2}, & S_i > K_{i,min} \end{cases} \tag{4.2}$$

In this equation, FAN and ammonium were both associated with inhibition parameters and jointly determined for an overall ammonia inhibition on the uptake of acetate reaction. The lower and upper inhibition limits were adjusted based on the ratio of solids concentration

with a study [19]. The results of this inhibition were implemented and best seen with the no acetate (0VFA) conditions with 0 g-N/L (0N) and 4 g-N/L at the neutral and high pH conditions (4N-NPH and 4N-HPH) as seen in Figure 4.5a. The 0N condition yielded more methane than 4N-NPH which yielded more methane than 4N-HPH. Compared to the 0VFA|0N experimental test, the model simulation methane reductions for 0N and 4N-NPH were 8% and 14%, respectively. For the 4N-NPH results, the model-to-experimental reduction was similar in final methane yield however, the 0N condition was underestimated. With little inhibition to the 0N test, this underestimation was then based on influent characterization for the amount of organic material and kinetic rates regarding the acetoclastic methanogenesis pathway to determine the lower rates of methanogenesis present, especially towards the second half of the test duration. The contribution of methane production from acetoclastic methanogens can be seen to decrease for increased FAN (Figure 4.6a, b, and c). The assumption of linear change in pH and ammonia likely contributed to the lack of correlation minimally.

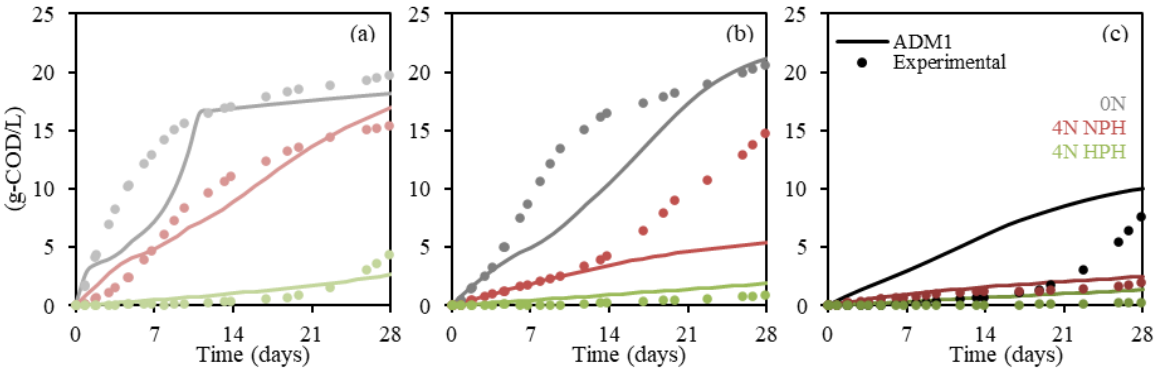

Figure 4.5: Methane production from ADM1 simulation results and experimental tests for: (a) no added acetate (0VFA), (b) 20 g-COD/L of added acetate (20VFA), and (c) 40 g-COD/L of added acetate (40VFA).

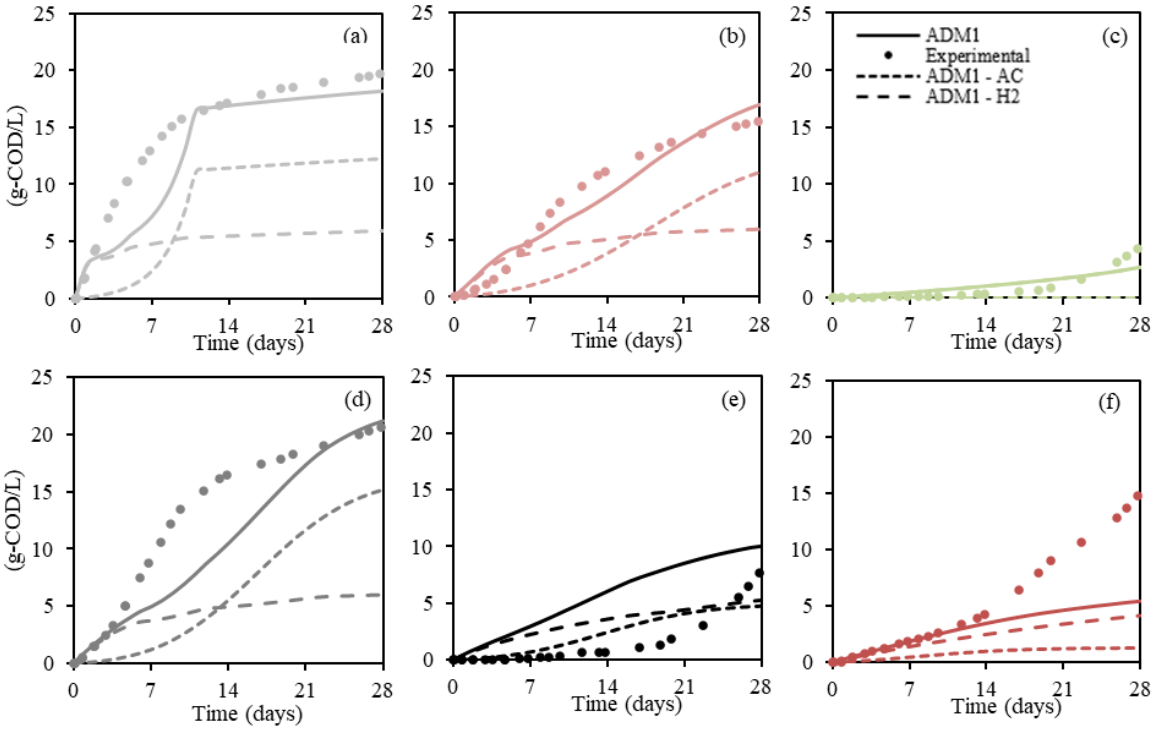

Figure 4.6: Methane production from acetoclastic and hydrogenotrophic methane contributions to ADM1 simulation results and experimental tests for: (a) 0VFA|0N, (b) 0VFA|4N-NPH, (c) 0VFA|4N-HPH, (d) 20VFA|0N, (e) 40VFA|0N, and (f) 20VFA|4N-NPH.

While acetoclastic methanogenesis is primarily involved with methane production, hydrogenotrophic methanogenesis was important to consider in the model for methane production and thus, ammonia inhibition. Here, a simple inhibition function for ammonia inhibition on hydrogenotrophic methanogens was implemented and fitted especially for the 4N conditions, Eq. (4.3):

$$I_{NH3,Xh2} = \frac{1}{1 + {S_{NH3}}/{K_{INH3,Xh2}}} \tag{4.3}$$

As seen in Figure 4.5a, the inhibition over the first few days decreases with increased FAN and inhibited methane production curves. Compared to the experimental tests, the model

simulation methane reductions for 4N-HPH compared to the 0N experimental test was 86% and thus the condition was underestimated. The gradual decrease in the initial methane production with increasing FAN is most associated to the hydrogenotrophic methanogen inhibition as seen in Figure 4.6a, b, and c. The presence of methane with the 4N-HPH condition is solely based on the minimal contribution by the hydrogenotrophic methanogens as acetoclastic methanogens are fully inhibited for this concentration of FAN. While the $K_{INH3,Xh2}$ value could have been minimally adjusted to represent the final methane yield, it was chosen to exemplify this methane simulation curve to represent the average methane yield throughout the duration for 4N-HPH while also contributing towards the lower rate of methanogenesis for 4N-HPH. Estimated inhibition parameters for the ammonia inhibition terms can be seen in Table 4.1. The assumed linear change of pH and ammonia concentrations was reflected in the 0VFA conditions as it caused underestimated values. This was present for most of the neutral pH tests' durations and was also observed towards the end of the high pH test. Overall, the trend of ammonia inhibition for the 0VFA tests was observed for both the experimental and ADM1 model results. This comparison verified the need for an added ammonia inhibition term for hydrogenotrophic methanogenesis and a modified inhibition term for acetoclastic methanogenesis that is specified to include toxicity effects from ammonia and ammonium.

Table 4.1: Estimated inhibition parameters for ammonia inhibition.

Eq.	Inhibition Type	Inhibition Parameters (g-N/L)
(4.1) & (4.2)	Free ammonia and ammonium inhibition on X_{AC} (Threshold Inhibition)	$K_{Imin,NH3} = 0.03$ $K_{Imax,NH3} = 0.36$ $K_{Imin,NH4} = 2.09$ $K_{Imax,NH4} = 13.4$
(4.3)	Free ammonia inhibition on X_{H2} (Simple Inhibition)	$K_{INH3,Xh2} = 7.0 \times 10^{-6}$

4.8 Model Simulations for Acetic Acid Inhibition with Ammonia Inhibition

There is no implementation of acetic acid inhibition terms in the generic ADM1 model. Thus, based on the 0, 20, and 40 g-COD/L (0VFA, 20VFA, and 40VFA) additions of acetate and the associated inhibitions observed through the experimental methane production graphs, three types of inhibition were implemented: (1) Haldane model for acetic acid inhibition on the uptake of acetate reaction (Eq. (4.4)), (2) simple inhibition model for acetic acid inhibition the same reaction (Eq. (4.5)), and (3) simple model for acetic acid inhibition on the uptake of hydrogen reaction (Eq. (4.6)):

$$r'_{11} = k_{ac} \frac{S_{AC}}{K_{sac} + S_{AC} + {S_{AC}^2}/{K_{IAC,Xac}}} X_{AC} I'_1 \tag{4.4}$$

$$I_{HAC,Xac} = \frac{1}{1 + {S_{HAC}}/{K_{IHAC,Xac}}} \tag{4.5}$$

$$I_{HAC,Xh2} = \frac{1}{1 + {S_{HAC}}/{K_{IHAC,Xh2}}} \tag{4.6}$$

The effects of the combined inhibitions can be best seen with the 0 g-N/L (0N) conditions with 0VFA, 20VFA, and 40VFA (Figure 4.5). All experimental results yielded the same final amount of methane as the model simulations for the increasing acetate conditions with 7% increase and 49% decrease compared to 0VFA for 20VFA and 40VFA, respectively. Overall, the same amount of methane was produced for all 0N tests.

Similar to its counterpart use with ammonia, the initial rates of methane production can be attributed to the acetic acid inhibition with the hydrogenotrophic methanogens as seen in Figure 4.6a, d, and e. For the 0N experimental tests, specifically 0VFA|0N, the hydrogen-, propionate- and butyrate-based fractions from sugars and amino acids were altered to observe a longer and more representative initial rate of methanogenesis from the hydrogenotrophic methanogens, unless inhibited by ammonia inhibition terms. The final methane yields were mostly enabled by the acetic acid inhibition terms regarding the acetoclastic methanogenesis pathways. The use of Haldane for the inhibition focused on the inhibition of the acetate uptake reaction at high acetate concentrations and the simple inhibition for acetic acid, which is less dominant at neutral and high pH conditions, resulted in similar inhibitions. Together, all these inhibitions observed the initial and final rates for acetoclastic methanogenesis. The 40VFA condition did not correlate accurately as hydrogenotrophic methanogens were not inhibited greatly, however, this inaccuracy could likely be due to the lack of duplicate values for the experimental component of this condition. It is generally observed that conditions with increased concentrations of acetate experienced decreased initial rates and increased final rates of methane production.

For the remaining conditions (4.5b, c) relating to 4 g-N/L at low and high pH conditions (4N-NPH and 4N-HPH) methane production was overestimated with a reduction of 90%, 87%, and 93% for 20VFA|4N-HPH, 40VFA|4N-NPH, and 40VFA|4N-HPH respectively, while it was largely underestimated for the 20VFA|4N-NPH condition at 72%. This outlier seemed to largely depend on the assumed linear change of pH and ammonia concentrations as the assumption was also observed for underestimated values in the 0VFA tests. Rate changes for most of the conditions are observed between 7-14 days but this change in the rate does not correlate with a change in pH or ammonia. In the case of 20VFA|4N-NPH, it was tested that a decrease in pH would observe a decrease in inhibition and thus an increase in the model output for methane production. Thus, a significant factor that is necessary for a better correlation between the experiment and simulation was to include more concentration and pH observations throughout the BMP test duration. Estimated inhibition parameters for the inhibition terms are listed (Table 4.2).

Table 4.2: Estimated inhibition parameters for acetic acid inhibition

Eq.	Inhibition Type	Inhibition Parameters (g-COD/L)
(4.4)	Acetic acid inhibition on $X_{AC,}$ acetoclastic methanogens (Haldane Inhibition)	$K_{IAC,Xac} = 85$
(4.5)	Acetic acid inhibition on XAC, acetoclastic methanogens (Simple Inhibition)	$K_{IHAC,Xac} = 0.5$
(4.6)	Acetic acid inhibition on X_{H2} hydrogenotrophic methanogens (Simple Inhibition)	$K_{IHAC,Xh2} = 0.015$

5 Conclusions

5.1 Ammonia and Acetic Acid Inhibition on High Solids Sludge

Based on experimental results with TWAS, ammonia was found to have a minor negative impact on methane production with a concentration of 4 g-N/L at a neutral pH but a major negative impact at a higher pH. This effect of inhibition was observed in TCOD reduction and an increased amount of solubilization. Acetic acid inhibition was found to have a major negative impact at the condition with 40 g-COD/L added acetate. The decreased VSS reduction, decreased TCOD reduction, and increase of sCOD indicated that issues influencing methanogenesis inhibition prevented soluble organic use at the increased acetate condition. The inhibited conditions that produced methane had high rates of methane production but resulted in a lower methane yield. Overall, it was observed that the more optimal yield in methane was exemplified for neutral pH conditions than high pH conditions for increased ammonia concentration tests and was more optimal for 0 g-COD/L and 20 g-COD/L added acetate conditions.

The model simulations of ADM1 observed how ammonia inhibition was required for both free ammonia and ammonium and how acetic acid inhibition was required for both acetate and acetic acid. These inhibitions were carried out to varying degrees for both acetoclastic and hydrogenotrophic methanogens. For acetoclastic methanogens, the use of threshold inhibition with ammonia observed inhibition for free ammonia and ammonium and was accurately modelled for the intermediate and final rates of methane production with the linear increase in pH and ammonia. Simple inhibitions for hydrogenotrophic methanogens was implemented to reduce the initial rate of methanogenesis for more

inhibited conditions with both free ammonia and acetic acid inhibitions. Acetic acid inhibitions were implemented for acetoclastic methanogens with simple inhibition and Haldane inhibition to better simulate the final methane yield. Though some conditions were not precisely modelled with these tests, the methane production rates and the final methane yields with increased ammonia and acetate conditions were accurately analysed, thus noting the best use of these required inhibition terms in modeling these conditions.

5.2 Recommendations for Future Work

There are several key research opportunities to build on this study and further understand the impacts of ammonia and acetic acid inhibition. To build on the model developed, future work can include modifications to a sampling procedure by obtaining measurements for pH, TAN and VFA throughout the experiment duration in order to improve the model for the intermediate sections of AD. While these tests are difficult to ascertain in batch BMP tests, they are necessary to determine the trend of pH change and its influence on TAN fractionation and VFA concentrations, thus supplying more data for more comprehensive model simulations. These concentrations could be measured when a change in rate of methane was observed or expected. Based on the results obtained, the model did not accurately fit with the experimental tests and would need to be verified, thus a duplicate test for the 40 g-COD/L conditions is necessary. Another area of research could be with the analysis of these batch experiments to produce enhanced kinetic coefficients, specifically for the Haldane acetic acid inhibition term and both simple inhibition terms regarding hydrogenotrophic methanogens. Alterations of model inputs for different substrates could be a future study to consider as integration of this ADM1 model would

eventually need to be applicable with different inputs and processes. In addition, the development of the model in steady-state conditions could be appropriate for the simulation of a continuously-run pilot study or full scale municipal anaerobic digester.

Future work for the experimental research components can also include studies of the effects of lower pH. By evaluating more pH ranges, parameters for ammonia inhibition regarding the threshold limits, and for acetic acid inhibition can be determined to improve AD efficiency. Acclimation of high organic conditions with increased ammonia content could also be another experimental work to consider as increased ammonia condition increased methane production. The comparison of these research ideas and this proposed research could look further into the effects of ammonia inhibition at higher acetate conditions. Some research into analysing acetic acid inhibition with varying neutral ranged pH values without ammonia would correspond to effects of pure organic addition, thus analysing inhibition effects for acetic acid for inhibition terms and comparing to those suggested in this study. Research into co-digestion of TWAS and an appropriate food waste substrate would also be an idea for implementation. Compared to TWAS, food waste would need to have similar solids concentrations, higher ammonia concentrations, and higher organic concentrations as outlined in these experiments without the addition of chemical components. Co-digestion would aid in finding the appropriate C/N ratio necessary for optimal methane production and this would also introduce a commonly-used strategy and scenario necessary for mitigating inhibition effects.

6 References

[1] Canadian Biogas Association, "Canadian Anaerobic Digestion Guideline," 2019.

[2] C. P. L. Grady, G. T. Daigger, N. G. Love and C. D. M. Filipe, Biological Wastewater Treatment, 3 ed., London: IWA Publishing, 2011.

[3] Y. Xu, Y. Lu, L. Zheng, Z. Wang and X. Dai, Perspective on enhancing the anaerobic digestion of waste activated sludge, vol. 389, Journal of Hazardous Materials, 2019.

[4] F. Xu, Y. Li, X. Ge, L. Yang and Y. Li, Anaerobic digestion of food waste – Challenges and opportunities, vol. 247, Bioresource Technology, 2017, pp. 1047-1058.

[5] A. Serna-Maza, S. Heaven and C. J. Banks, Ammonia removal in food waste anaerobic digestion using a side-stream stripping process, vol. 152, Bioresource Technology, 2014, pp. 307-315.

[6] J. Vermeulen, A. Huysmans, M. Crespo, A. Van Lierde, A. De Rycke and W. Verstraete, Processing of Biowaste by Anaerobic Composting to Plant Growth Substrates, vol. 27, Water Science and Technology, 1993, pp. 109-119.

[7] A. Khalid, M. Arshad, M. Anjum, T. Mahmood and L. Dawson, The anaerobic digestion of solid organic waste, vol. 31, Waste Management, 2011, pp. 1737-1744.

[8] O. Yenigun and B. Demirel, Ammonia inhibition in anaerobic digestion: A review, vol. 48, Process Biochemistry, 2019, pp. 901-911.

[9] "Ontario's Food and Organic Waste Framework: Action Plan," Ontario Ministry of the Environment and Climate Change, 2017.

[10] P. L. McCarty, "Anaerobic Waste Treatment Fundamentals III," Public Works, 1964.

[11] B. Demirel and P. Scherer, The roles of acetotrophic and hydrogenotrophic methanogens during anaerobic conversion of biomass to methane: a review, vol. 7, Environmental Science, 2008, pp. 173-190.

[12] Y. Chen, J. J. Cheng and K. S. Creamer, "Inhibition of anaerobic digestion process: A review," Bioresource Technology, 2007.

[13] R. Zhang, H. M. El-Mashad, K. Hartman, F. Wang, G. Liu, C. Choate and P. Gamble, Characterization of food waste as feedstock for anaerobic digestion, vol. 98, Bioresource Technology, 2007, pp. 929-935.

[14] D.-J. Lee, S.-Y. Lee, J.-S. Bae, J.-G. Kang, K.-H. Kim, S.-S. Rhee, J.-H. Park, J.-S. Cho, J. Chung and D.-C. Seo, Effect of Volatile Fatty Acid Concentration on Anaerobic Degradation Rate from Field Anaerobic Digestion Facilities Treating Food Waste Leachate in South Korea, Journal of Chemistry, 2015.

[15] J.-J. Lay, Y.-Y. Li and T. Noike, The influence of pH and ammonia concentration on the methane prodution in high-solids digestion processes, vol. 70, Water Environment Research, 1998.

[16] C.-f. Liu, X.-z. Yuan, G.-m. Zeng, W.-w. Li and J. Li, Prediction of methane yield at optimum pH for anaerobic digestion, vol. 99, Bioresource Technology, 2008, pp. 882-888.

[17] I. Angelidaki and B. K. Ahring, Thermophilic anaerobic digestion of livestock waste: the effect of ammonia, vol. 38, Applied Microbiology and Biotechnology, 1992, pp. 560-564.

[18] Y. Jiang, E. McAdam, Y. Zhang, S. Heaven, C. Banks and L. Philip, Ammonia Inhibition and toxicity in anaerobic digestion: A critical review, vol. 32, Journal of Water Process Engineering, 2019.

[19] S. Astals, M. Peces, D. J. Batstone, P. D. Jensen and S. Tait, Characterising and modelling free ammonia and ammonium inhibition in anaerobic systems, vol. 143, Water Research, 2018, pp. 127-135.

[20] H. Poggi-Varaldo, R. Rodriguez-Vazquez, G. Fernandez-Villagomez and F. Esparza-Garcia, Inhibition of mesophilic solid-substrate anaerobic digestion by ammonia nitrogen, vol. 47, Applications of Microbiology Biotechnology, 1997, pp. 284-291.

[21] H. V. Hendriksen and K. B. Ahring, Effects of ammonia on growth and morphology of thermophilic hydrogen-oxidizing methanogenic bacteria, vol. 85, FEMS Microbiology Ecology, 1991, pp. 241-246.

[22] A. F. M. Van Velsen, Adaptation of methanogenic sludge to high ammonia-nitrogen concentrations, vol. 13, Water Research, 1979, pp. 995-999.

[23] I. A. Fotidis, D. Karakashev, T. A. Kotsopoulos, G. G. Martzopoulos and I. Angelidaki, Effect of ammonium and acetate on methanogenic pathway and

methanogenic community composition, vol. 83, FEMS Microbiology Ecology, 2013, pp. 38-48.

[24] I. H. Franke-Whittle, A. Walter, C. Ebner and H. Insam, Investigation into the effect of high concentrations of volatile fatty acids, vol. 34, Waste Management, 2014, pp. 2080-2089.

[25] T. Dogan, O. Ince, N. A. Oz and B. K. Ince, Inhibition of Volatile Fatty Acid Production in Granular Sludge form a UASB Reactor, vol. 40, Journal of Environmental Science and Health, 2005, pp. 633-644.

[26] X. Li, Z. Yang, G. Liu, Z. Ma and W. Wang, Modified anaerobic digestion model No.1 (ADM1) for modeling anaerobic digestion process at different ammonium concentrations, vol. 91, Water Environment Research, 2019, pp. 700-714.

[27] W. M. Wiegant and G. Zeeman, The Mechanism of Ammonia Inhibition in the Thermophilic Digestion of Livestock Wastes, vol. 16, Agricultural Wastes, 1986, pp. 243-253.

[28] D. J. Batstone, J. Keller, I. Angelidaki, S. V. Kalyuzhnyi, S. G. Pavlostathis, A. Rozzi, W. T. Sanders, H. Siegrist and V. A. Vavilin, "The IWA Anaerobic Digestion Model No 1 (ADM1)," Water Science and Technology, 2002.

[29] D. Batstone, J. Keller and J. Steyer, "A review of ADM1 extensions, applications, and analysis: 2002-2005," 2006.

[30] B. Fezzani and R. B. Cheikh, Implementation of IWA anaerobic digestion model No. 1 (ADM1) for simulation the thermophilic anaerobic co-digestion of olive mill wastewater with olive mill solid waste in a semi-continuous tubular digester, Chemical Engineering Journal, 2008, pp. 75-88.

[31] W. F. Owen, D. C. Stuckey, J. B. Healy, L. Y. Young and P. L. McCarty, "Bioassay for Monitoring Biochemical Methane Potential and Anaerobic Toxicity," Water Research, 1978.

[32] D. J. Batstone, S. Tait and D. Starrenburg, Estimation of Hydrolysis Parameters in Full-Scale Anaerobic DIgesters, vol. 102, Biotechnology and Bioengineering, 2009, pp. 1513-1520.

[33] APHA, AWWA, WEF, STANDARD METHODS FOR THE EXAMINATION OF WATER AND WASTEWATER, 23 ed., E. W. Rice, R. B. Baird and A. D. Eaton, Eds., American Public Health Association, American Water Works Association, Water Environment Federation, 2017.

[34] O. Bernard, Z. Hadj-Sadok, D. Dochain, A. Genovesi and J.-P. Steyer, Dynamical Model Development and Parameter Identification for an Anaerobic Wastewater Treatment Process, vol. 75, Biotechnology and Bioengineering, 2001, pp. 424-438.

[35] L. Y. Lokshina, V. A. Vavilin, R. H. Kettunen, J. A. Rintala, C. Holliger and A. N. Nozhevnikova, Evaluation of kinetic coefficients using integrated Monod and Haldane models for low-temperature acetoclastic methanogenesis, vol. 35, Water Research, 2001, pp. 2913-2922.

[36] Y. Hirmiz, Y. Hong and Y. Kim, "A new model with serial hydrolysis reactions for the anaerobic digestion of waste activated sludge under thermophilic conditions," Environmental Science Water Research & Technology, 2019.

[37] C. Rosen and U. Jeppsson, "Aspects on ADM1 Implementation within the BSM2 Framework," Department of Industrial Electrical Engineering and Automation, Lund University, Lund, 2006.

[38] A. Aguilar, C. Casas and J. M. Lema, Degradation of Volatile Fatty Acids By Differently Enriched Methanogenic Cultures: Kinetics and Inhibition, vol. 29, Water Research, 1995, pp. 505-509.

[39] I. Owusu-Agyeman, E. Plaza and Z. Cetecioglu, Production of volatile fatty acids through co-digestion of sewage sludge and external organic waste: Effect of substrate proportions and long-term operation, vol. 112, Waste Management, 2020, pp. 30-39.

[40] S. Sung and T. Liu, Ammonia inhibition on thermophilic anaerobic digestion, vol. 53, Chemosphere, 2003, pp. 43-52.

[41] H. Tian, I. A. Fotidis, K. Kissas and I. Angelidaki, Effect of different ammonia sources on aceticlastic and hydrogenotrophic methanogens, vol. 250, Bioresource Technology, 2018, pp. 390-397.

[42] A. A. Akindele and M. Sartaj, The toxicity effects of ammonia on anaerobic digestion of organic fraction of municipal solid waste, vol. 71, Waste Management, 2018, pp. 757-766.

[43] C. Veluchamy and A. S. Kalamdhad, Biochemical methane potential test for pulp and paper mill sludge with different food to microorganisms ratios and its kinetics, vol. 117, International Biodeterioration & Biodegradation, 2017, pp. 197-204.

Appendix A: Non-Steady State Equations

For all Mass Balances, based on batch reactor:

$$[Change] = [In] - [Out] + [Reaction]$$

Soluble Components

A.1 Mass balance on soluble sugars S_{su}

$$V * \left(\frac{dS_{su}}{dt}\right) = Q * S_{su,in} - Q * S_{su} + V * \left[(r_2) + \left(1 - f_{fali}\right) * (r_4) - (r_5)\right]$$

$$V * \left(\frac{dS_{su}}{dt}\right) = Q * S_{su,in} - Q * S_{su} + V * \left[1 * (k_{hyd,ch} * X_{ch}) + (1 - f_{fa,li}) * (k_{hyd,li} * X_{li}) - 1 * (k_{su} * \frac{S_{su}}{K_{s,su} + S_{su}} * X_{su} * I_1)\right]$$

$$V * \left(\frac{dS_{su}}{dt}\right) = V * \left[(k_{hyd,ch} * X_{ch}) + (1 - f_{fa,li}) * (k_{hyd,li} * X_{li}) - (k_{su} * \frac{S_{su}}{K_{s,su} + S_{su}} * X_{su} * I_1)\right]$$

$$S_{su(1)} = S_{su(0)} + \Delta t * \left[(k_{hyd,ch} * X_{ch(1)}) + (1 - f_{fa,li}) * (k_{hyd,li} * X_{li(1)}) - (k_{su} * \frac{S_{su(1)}}{K_{s,su} + S_{su(1)}} * X_{su(1)} * I_1\right]$$

$$\boldsymbol{S_{su(1)} = \frac{S_{su(0)} + \Delta t * \left[(k_{hyd,ch} * X_{ch(1)}) + (1 - f_{fa,li}) * (k_{hyd,li} * X_{li(1)})\right]}{1 + \Delta t * (k_{su} * \frac{1}{K_{s,su} + S_{su(1)}} * X_{su(1)} * I_{ph1} I_{IN,\mathrm{lim}})}}$$

A. 2 Mass balance on soluble amino acids S_{aa}

$$V * \left(\frac{dS_{aa}}{dt}\right) = Q * S_{aa,in} - Q * S_{aa} + V * [r_3 - r_6]$$

$$V * \left(\frac{dS_{aa}}{dt}\right) = Q * S_{aa,in} - Q * S_{aa} + V * \left[1 * (k_{hyd,pr} * X_{pr}) - 1 * (k_{aa} * \frac{S_{aa}}{K_{s,aa} + S_{aa}} * X_{aa} * I_1)\right]$$

$$V * \left(\frac{dS_{aa}}{dt}\right) = V * \left[(k_{hyd,pr} * X_{pr}) - (k_{aa} * \frac{S_{aa}}{K_{s,aa} + S_{aa}} * X_{aa} * I_1)\right]$$

$$S_{aa(1)} = S_{aa(0)} + \Delta t * \left[(k_{hyd,pr} * X_{pr(1)}) - (k_{aa} * \frac{S_{aa(1)}}{K_{s,aa} + S_{aa(1)}} * X_{aa(1)} * I_1)\right]$$

$$\boldsymbol{S_{aa(1)} = \frac{S_{aa(0)} + \Delta t * \left[(k_{hyd,pr} * X_{pr(1)})\right]}{1 + \Delta t * (k_{aa} * \frac{1}{K_{s,aa} + S_{aa(1)}} * X_{aa(1)} * I_{ph1} I_{IN,\lim})}}$$

A. 3 Mass balance on soluble fatty acids S_{fa}

$$V * \left(\frac{dS_{fa}}{dt}\right) = Q * S_{fa,in} - Q * S_{fa} + V * \left[f_{fa,li} * r_4 - r_7\right]$$

$$V * \left(\frac{dS_{fa}}{dt}\right) = Q * S_{fa,in} - Q * S_{fa} + V * \left[f_{fa,li} * (k_{hyd,li} * X_{li}) - 1 * (k_{fa} * \frac{S_{fa}}{K_{s,fa} + S_{fa}} * X_{fa} * I_2)\right]$$

$$V * \left(\frac{dS_{fa}}{dt}\right) = V * \left[f_{fa,li} * (k_{hyd,li} * X_{li}) - (k_{fa} * \frac{S_{fa}}{K_{s,fa} + S_{fa}} * X_{fa} * I_2)\right]$$

$$S_{fa(1)} = S_{fa(0)} + \Delta t * \left[f_{fa,li} * (k_{hyd,li} * X_{li(1)}) - (k_{fa} * \frac{S_{fa(1)}}{K_{s,fa} + S_{fa(1)}} * X_{fa(1)} * I_2)\right]$$

$$\boldsymbol{S_{fa(1)} = \frac{S_{fa(0)} + \Delta t * \left[f_{fa,li} * (k_{hyd,li} * X_{li(1)})\right]}{1 + \Delta t * (k_{fa} * \frac{1}{K_{s,fa} + S_{fa(1)}} * X_{fa(1)} * I_{ph1} I_{IN,\lim} \frac{K_{Ih2fa}}{K_{Ih2fa} + S_{h2(1)}})}}$$

A. 4 Mass balance on soluble valerate S_{va}

$$V * \left(\frac{dS_{va}}{dt}\right) = Q * S_{va,in} - Q * S_{va} + V * \left[(1 - Y_{aa}) * f_{va,aa} * r_6 - r_8\right]$$

$$V * \left(\frac{dS_{va}}{dt}\right) = Q * S_{va,in} - Q * S_{va} + V * \left[(1 - Y_{aa}) * f_{va,aa} * \left(k_{aa} * \frac{S_{aa}}{K_{s,aa} + S_{aa}} * X_{aa} * I_1\right) - \left(k_{c4} * \frac{S_{va}}{K_{s,c4} + S_{va}} * X_{c4} * \frac{S_{va}}{S_{va} + S_{bu}} * I_2\right)\right]$$

$$V * \left(\frac{dS_{va}}{dt}\right) = V * \left[(1 - Y_{aa}) * f_{va,aa} * \left(k_{aa} * \frac{S_{aa}}{K_{s,aa} + S_{aa}} * X_{aa} * I_1\right) - \left(k_{c4} * \frac{S_{va}}{K_{s,c4} + S_{va}} * X_{c4} * \frac{S_{va}}{S_{va} + S_{bu}} * I_2\right)\right]$$

$$S_{va(1)} = S_{va(0)} + \Delta t * \left[(1 - Y_{aa}) * f_{va,aa} * \left(k_{aa} * \frac{S_{aa(1)}}{K_{s,aa} + S_{aa(1)}} * X_{aa(1)} * I_1\right) - \left(k_{c4} * \frac{S_{va(1)}}{K_{s,c4} + S_{va(1)}} * X_{c4(1)} * \frac{S_{va(1)}}{S_{va(1)} + S_{bu(1)}} * I_2\right)\right]$$

$$\boldsymbol{S_{va(1)} = \frac{S_{va(0)} + \Delta t * \left[(1 - Y_{aa}) * f_{va,aa} * \left(k_{aa} * \frac{S_{aa(1)}}{K_{s,aa} + S_{aa(1)}} * X_{aa(1)} * I_{ph1} I_{IN,\lim}\right)\right]}{1 + \Delta t * \left(k_{c4} * \frac{1}{K_{s,c4} + S_{va(1)}} * X_{c4(1)} * \frac{S_{va(1)}}{S_{va(1)} + S_{bu(1)}} * I_{ph1} I_{IN,\lim} \frac{K_{Ih2c4}}{K_{Ih2c4} + S_{h2(1)}}\right)}}$$

A. 5 Mass balance on soluble butyrate S_{bu}

$$V * \left(\frac{dS_{bu}}{dt}\right) = Q * S_{bu,in} - Q * S_{bu} + V * \left[(1 - Y_{su}) * f_{bu,su} * r_5 + (1 - Y_{aa}) * f_{bu,aa} * r_6 - r_9\right]$$

$$V * \left(\frac{dS_{bu}}{dt}\right) = Q * S_{bu,in} - Q * S_{bu} + V * \left[(1 - Y_{su}) * f_{bu,su} * (k_{su} * \frac{S_{su}}{K_{s,su} + S_{su}} * X_{su} * I_1) + (1 - Y_{aa}) * f_{bu,aa} * \left(k_{aa} * \frac{S_{aa}}{K_{s,aa} + S_{aa}} * X_{aa} * I_1\right) - \left(k_{c4} * \frac{S_{bu}}{K_{s,c4} + S_{bu}} * X_{c4} * \frac{S_{bu}}{S_{va} + S_{bu}} * I_2\right)\right]$$

$$V * \left(\frac{dS_{bu}}{dt}\right) = V * \left[(1 - Y_{su}) * f_{bu,su} * (k_{su} * \frac{S_{su}}{K_{s,su} + S_{su}} * X_{su} * I_1) + (1 - Y_{aa}) * f_{bu,aa} * \left(k_{aa} * \frac{S_{aa}}{K_{s,aa} + S_{aa}} * X_{aa} * I_1\right) - \left(k_{c4} * \frac{S_{bu}}{K_{s,c4} + S_{bu}} * X_{c4} * \frac{S_{bu}}{S_{va} + S_{bu}} * I_2\right)\right]$$

$$S_{bu(1)} = S_{bu(0)} + \Delta t * \left[(1 - Y_{su}) * f_{bu,su} * (k_{su} * \frac{S_{su(1)}}{K_{s,su} + S_{su(1)}} * X_{su(1)} * I_1) + (1 - Y_{aa}) * f_{bu,aa} * \left(k_{aa} * \frac{S_{aa(1)}}{K_{s,aa} + S_{aa(1)}} * X_{aa(1)} * I_1\right) - \left(k_{c4} * \frac{S_{bu(1)}}{K_{s,c4} + S_{bu(1)}} * X_{c4(1)} * \frac{S_{bu(1)}}{S_{va(1)} + S_{bu(1)}} * I_2\right)\right]$$

$$\boldsymbol{S_{bu(1)} = \frac{S_{bu(0)} + \Delta t * \left(\begin{array}{c}(1-Y_{su}) * f_{bu,su} * \left(k_{su} * \frac{S_{su(1)}}{K_{s,su}+S_{su(1)}} * X_{su(1)} * I_{ph1} I_{IN,\lim}\right) \\ +(1-Y_{aa}) * f_{bu,aa} * \left(k_{aa} * \frac{S_{aa(1)}}{K_{s,aa}+S_{aa(1)}} * X_{aa(1)} * I_{ph1} I_{IN,\lim}\right)\end{array}\right)}{1 + \Delta t * \left(k_{c4} * \frac{1}{K_{s,c4} + S_{bu(1)}} * X_{c4(1)} * \frac{S_{bu(1)}}{S_{va(1)} + S_{bu(1)}} * I_{ph1} I_{IN,\lim} \frac{K_{Ih2c4}}{K_{Ih2c4} + S_{h2(1)}}\right)}}$$

A. 6 Mass balance on soluble propionate S_{pro}

$$V * \left(\frac{dS_{pro}}{dt}\right) = Q * S_{pro,in} - Q * S_{pro} + V * \left[(1 - Y_{su}) * f_{pro,su} * r_5 + (1 - Y_{aa}) * f_{pro,aa} * r_6 + (1 - Y_{c4}) * 0.54 * r_8 - r_{10}\right]$$

$$V * \left(\frac{dS_{pro}}{dt}\right) = Q * S_{pro,in} - Q * S_{pro} + V * \left[(1 - Y_{su}) * f_{pro,su} * \left(k_{su} * \frac{S_{su}}{K_{s,su} + S_{su}} * X_{su} * I_1\right) + (1 - Y_{aa}) * f_{pro,aa} * \left(k_{aa} * \frac{S_{aa}}{K_{s,aa} + S_{aa}} * X_{aa} * I_1\right) + (1 - Y_{c4})0.54 * \left(k_{c4} * \frac{S_{va}}{K_{s,c4} + S_{va}} * X_{c4} * \frac{S_{va}}{S_{va} + S_{bu}} * I_2\right) - \left(k_{pro} * \frac{S_{pro}}{K_{s,pro} + S_{pro}} * X_{pro} * I_2\right)\right]$$

$$V * \left(\frac{dS_{pro}}{dt}\right) = V * \left[(1 - Y_{su}) * f_{pro,su} * \left(k_{su} * \frac{S_{su}}{K_{s,su} + S_{su}} * X_{su} * I_1\right) + (1 - Y_{aa}) * f_{pro,aa} * \left(k_{aa} * \frac{S_{aa}}{K_{s,aa} + S_{aa}} * X_{aa} * I_1\right) + (1 - Y_{c4})0.54 * \left(k_{c4} * \frac{S_{va}}{K_{s,c4} + S_{va}} * X_{c4} * \frac{S_{va}}{S_{va} + S_{bu}} * I_2\right) - \left(k_{pro} * \frac{S_{pro}}{K_{s,pro} + S_{pro}} * X_{pro} * I_2\right)\right]$$

$$S_{pro(1)} = S_{pro(0)} + \Delta t * \left[(1 - Y_{su}) * f_{pro,su} * \left(k_{su} * \frac{S_{su(1)}}{K_{s,su} + S_{su(1)}} * X_{su(1)} * I_1\right) + (1 - Y_{aa}) * f_{pro,aa} * \left(k_{aa} * \frac{S_{aa(1)}}{K_{s,aa} + S_{aa(1)}} * X_{aa(1)} * I_1\right) + (1 - Y_{c4})0.54 * \left(k_{c4} * \frac{S_{va(1)}}{K_{s,c4} + S_{va(1)}} * X_{c4(1)} * \frac{S_{va(1)}}{S_{va(1)} + S_{bu(1)}} * I_2\right) - \left(k_{pro} * \frac{S_{pro(1)}}{K_{s,pro} + S_{pro(1)}} * X_{pro(1)} * I_2\right)\right]$$

$$S_{pro(1)} = \frac{S_{pro(0)} + \Delta t * \begin{pmatrix} (1-Y_{su}) * f_{pro,su} * \left(k_{su} * \frac{S_{su(1)}}{K_{s,su}+S_{su(1)}} * X_{su(1)} * I_{ph1} I_{IN,\lim}\right) \\ +(1-Y_{aa}) * f_{pro,aa} * \left(k_{aa} * \frac{S_{aa(1)}}{K_{s,aa}+S_{aa(1)}} * X_{aa(1)} * I_{ph1} I_{IN,\lim}\right) \\ +(1-Y_{c4}) 0.54 * \left(k_{c4} * \frac{S_{va(1)}}{K_{s,c4}+S_{va(1)}} * X_{c4(1)} * \frac{S_{va(1)}}{S_{va(1)}+S_{bu(1)}} * I_{ph1} I_{IN,\lim} \frac{K_{Ih2c4}}{K_{Ih2c4}+S_{h2(1)}}\right) \end{pmatrix}}{\left(1 + \Delta t * \left(k_{pro} * \frac{1}{K_{s,pro}+S_{pro(1)}} * X_{pro(1)} * I_{ph1} I_{IN,\lim} \frac{K_{Ih2pro}}{K_{Ih2pro}+S_{h2(1)}}\right)\right)}$$

A. 7 Mass balance on soluble acetate S_{ac}

$$V * \left(\frac{dS_{ac}}{dt}\right) = Q * S_{ac,in} - Q * S_{ac} + V * \left[(1 - Y_{su}) * f_{ac,su} * r_5 + (1 - Y_{aa}) * f_{ac,aa} * r_6 + (1 - Y_{fa}) * 0.7 * r_7 + (1 - Y_{c4}) * 0.31 * r_8 + (1 - Y_{c4}) * 0.8 * r_9 + (1 - Y_{pro}) * 0.57 * r_{10} - r'_{11}\right]$$

$$V * \left(\frac{dS_{ac}}{dt}\right) = Q * S_{ac,in} - Q * S_{ac} + V$$
$$* \left[(1 - Y_{su}) * f_{ac,su} * \left(k_{su} * \frac{S_{su}}{K_{s,su} + S_{su}} * X_{su} * I_1 \right) + (1 - Y_{aa}) * f_{ac,aa} * \left(k_{aa} * \frac{S_{aa}}{K_{s,aa} + S_{aa}} * X_{aa} * I_1 \right) \right.$$
$$+ (1 - Y_{c4})0.7 * \left(k_{fa} * \frac{S_{fa}}{K_{s,fa} + S_{fa}} * X_{fa} * I_2 \right) + (1 - Y_{c4})0.31 * \left(k_{c4} * \frac{S_{va}}{K_{s,c4} + S_{va}} * X_{c4} * \frac{S_{va}}{S_{va} + S_{bu}} * I_2 \right)$$
$$+ (1 - Y_{c4})0.8 * \left(k_{c4} * \frac{S_{bu}}{K_{s,c4} + S_{bu}} * X_{c4} * \frac{S_{bu}}{S_{va} + S_{bu}} * I_2 \right) + (1 - Y_{pro})0.57$$
$$\left. * \left(k_{pro} * \frac{S_{pro}}{K_{s,pro} + S_{pro}} * X_{pro} * I_2 \right) - \left(k_{ac} * \frac{S_{ac}}{K_{s,ac} + S_{ac} + {S_{ac}^2}/{K_{IAC,Xac}}} * X_{ac} * I_3' \right) \right]$$

$$V * \left(\frac{dS_{ac}}{dt}\right) = V$$
$$* \left[(1 - Y_{su}) * f_{ac,su} * \left(k_{su} * \frac{S_{su}}{K_{s,su} + S_{su}} * X_{su} * I_1 \right) + (1 - Y_{aa}) * f_{ac,aa} * \left(k_{aa} * \frac{S_{aa}}{K_{s,aa} + S_{aa}} * X_{aa} * I_1 \right) \right.$$
$$+ (1 - Y_{c4})0.7 * \left(k_{fa} * \frac{S_{fa}}{K_{s,fa} + S_{fa}} * X_{fa} * I_2 \right) + (1 - Y_{c4})0.31 * \left(k_{c4} * \frac{S_{va}}{K_{s,c4} + S_{va}} * X_{c4} * \frac{S_{va}}{S_{va} + S_{bu}} * I_2 \right)$$
$$+ (1 - Y_{c4})0.8 * \left(k_{c4} * \frac{S_{bu}}{K_{s,c4} + S_{bu}} * X_{c4} * \frac{S_{bu}}{S_{va} + S_{bu}} * I_2 \right) + (1 - Y_{pro})0.57$$
$$\left. * \left(k_{pro} * \frac{S_{pro}}{K_{s,pro} + S_{pro}} * X_{pro} * I_2 \right) - \left(k_{ac} * \frac{S_{ac}}{K_{s,ac} + S_{ac} + {S_{ac}^2}/{K_{IAC,Xac}}} * X_{ac} * I_3' \right) \right]$$

$$S_{ac(1)} = S_{ac(0)} + \Delta t$$
$$* \left[(1 - Y_{su}) * f_{ac,su} * \left(k_{su} * \frac{S_{su(1)}}{K_{s,su} + S_{su(1)}} * X_{su(1)} * I_1 \right) + (1 - Y_{aa}) * f_{ac,aa} \right.$$
$$* \left(k_{aa} * \frac{S_{aa(1)}}{K_{s,aa} + S_{aa(1)}} * X_{aa(1)} * I_1 \right) + (1 - Y_{c4})0.7 * \left(k_{fa} * \frac{S_{fa(1)}}{K_{s,fa} + S_{fa(1)}} * X_{fa(1)} * I_2 \right) + (1 - Y_{c4})0.31$$
$$* \left(k_{c4} * \frac{S_{va(1)}}{K_{s,c4} + S_{va(1)}} * X_{c4(1)} * \frac{S_{va(1)}}{S_{va(1)} + S_{bu(1)}} * I_2 \right) + (1 - Y_{c4})0.8$$
$$* \left(k_{c4} * \frac{S_{bu(1)}}{K_{s,c4} + S_{bu(1)}} * X_{c4(1)} * \frac{S_{bu(1)}}{S_{va(1)} + S_{bu(1)}} * I_2 \right) + (1 - Y_{pro})0.57$$
$$\left. * \left(k_{pro} * \frac{S_{pro(1)}}{K_{s,pro} + S_{pro(1)}} * X_{pro(1)} * I_2 \right) - \left(k_{ac} * \frac{S_{ac(1)}}{K_{s,ac} + S_{ac(1)} + {S_{ac(1)}^2}/{K_{IAC,Xac}}} * X_{ac(1)} * I_3' \right) \right]$$

$$S_{ac(1)} = \frac{S_{ac(0)} + \Delta t * \left(\begin{array}{c} (1 - Y_{su}) * f_{ac,su} * \left(k_{su} * \frac{S_{su(1)}}{K_{s,su} + S_{su(1)}} * X_{su(1)} * I_{ph1} I_{IN,\lim} \right) \\ +(1 - Y_{aa}) * f_{ac,aa} * \left(k_{aa} * \frac{S_{aa(1)}}{K_{s,aa} + S_{aa(1)}} * X_{aa(1)} * I_{ph1} I_{IN,\lim} \right) \\ +(1 - Y_{c4}) 0.7 * \left(k_{fa} * \frac{S_{fa(1)}}{K_{s,fa} + S_{fa(1)}} * X_{fa(1)} * I_{ph1} I_{IN,\lim} \frac{K_{Ih2fa}}{K_{Ih2fa} + S_{h2(1)}} \right) \\ +(1 - Y_{c4}) 0.31 * \left(k_{c4} * \frac{S_{va(1)}}{K_{s,c4} + S_{va(1)}} * X_{c4} * \frac{S_{va(1)}}{S_{va(1)} + S_{bu(1)}} * I_{ph1} I_{IN,\lim} \frac{K_{Ih2c4}}{K_{Ih2c4} + S_{h2(1)}} \right) \\ +(1 - Y_{c4}) 0.8 * \left(k_{c4} * \frac{S_{bu(1)}}{K_{s,c4} + S_{bu(1)}} * X_{c4(1)} * \frac{S_{bu(1)}}{S_{va(1)} + S_{bu(1)}} * I_{ph1} I_{IN,\lim} \frac{K_{Ih2c4}}{K_{Ih2c4} + S_{h2(1)}} \right) \\ +(1 - Y_{pro}) 0.57 * \left(k_{pro} * \frac{S_{pro(1)}}{K_{s,pro} + S_{pro(1)}} * X_{pro(1)} * I_{ph1} I_{IN,\lim} \frac{K_{Ih2pro}}{K_{Ih2pro} + S_{h2(1)}} \right) \end{array} \right)}{1 + \Delta t * \left(k_{ac} * \frac{1}{K_{s,ac} + S_{ac(1)} + {S_{ac(1)}^2}/{K_{IAC,Xac}}} * X_{ac(1)} * I_{ph2} I_{IN,\lim} I_{NH,Xac} I_{HAC,Xac} \right)}$$

A. 8 Mass balance on hydrogen gas S_{h2}

$$V * \left(\frac{dS_{h2}}{dt} \right) = Q * S_{h2,in} - Q * S_{h2} + V * \left[(1 - Y_{su}) * f_{h2,su} * r_5 + (1 - Y_{aa}) * f_{h2,aa} * r_6 + (1 - Y_{fa}) * 0.3 * r_7 + (1 - Y_{c4}) * 0.15 * r_8 + (1 - Y_{c4}) * 0.2 * r_9 + (1 - Y_{pro}) * 0.43 * r_{10} - r'_{12} \right]$$

$$V * \left(\frac{dS_{h2}}{dt}\right) = Q * S_{h2,in} - Q * S_{h2} + V$$
$$* \left[(1 - Y_{su}) * f_{h2,su} * \left(k_{su} * \frac{S_{su}}{K_{s,su} + S_{su}} * X_{su} * I_1\right) + (1 - Y_{aa}) * f_{h2,aa} * \left(k_{aa} * \frac{S_{aa}}{K_{s,aa} + S_{aa}} * X_{aa} * I_1\right)\right.$$
$$+ (1 - Y_{c4})0.3 * \left(k_{fa} * \frac{S_{fa}}{K_{s,fa} + S_{fa}} * X_{fa} * I_2\right) + (1 - Y_{c4})0.15 * \left(k_{c4} * \frac{S_{va}}{K_{s,c4} + S_{va}} * X_{c4} * \frac{S_{va}}{S_{va} + S_{bu}} * I_2\right)$$
$$+ (1 - Y_{c4})0.2 * \left(k_{c4} * \frac{S_{bu}}{K_{s,c4} + S_{bu}} * X_{c4} * \frac{S_{bu}}{S_{va} + S_{bu}} * I_2\right) + (1 - Y_{pro})0.43$$
$$\left. * \left(k_{pro} * \frac{S_{pro}}{K_{s,pro} + S_{pro}} * X_{pro} * I_2\right) - \left(k_{h2} * \frac{S_{h2}}{K_{s,h2} + S_{h2}} * X_{h2} * I_1'\right)\right]$$

$$V * \left(\frac{dS_{h2}}{dt}\right) = V$$
$$* \left[(1 - Y_{su}) * f_{h2,su} * \left(k_{su} * \frac{S_{su}}{K_{s,su} + S_{su}} * X_{su} * I_1\right) + (1 - Y_{aa}) * f_{h2,aa} * \left(k_{aa} * \frac{S_{aa}}{K_{s,aa} + S_{aa}} * X_{aa} * I_1\right)\right.$$
$$+ (1 - Y_{c4})0.3 * \left(k_{fa} * \frac{S_{fa}}{K_{s,fa} + S_{fa}} * X_{fa} * I_2\right) + (1 - Y_{c4})0.15 * \left(k_{c4} * \frac{S_{va}}{K_{s,c4} + S_{va}} * X_{c4} * \frac{S_{va}}{S_{va} + S_{bu}} * I_2\right)$$
$$+ (1 - Y_{c4})0.2 * \left(k_{c4} * \frac{S_{bu}}{K_{s,c4} + S_{bu}} * X_{c4} * \frac{S_{bu}}{S_{va} + S_{bu}} * I_2\right) + (1 - Y_{pro})0.43$$
$$\left. * \left(k_{pro} * \frac{S_{pro}}{K_{s,pro} + S_{pro}} * X_{pro} * I_2\right) - \left(k_{h2} * \frac{S_{h2}}{K_{s,h2} + S_{h2}} * X_{h2} * I_1'\right)\right]$$

$$S_{h2(1)} = S_{h2(0)} + \Delta t$$
$$* \left[(1 - Y_{su}) * f_{h2,su} * \left(k_{su} * \frac{S_{su(1)}}{K_{s,su} + S_{su(1)}} * X_{su(1)} * I_1 \right) + (1 - Y_{aa}) * f_{h2,aa} \right.$$
$$* \left(k_{aa} * \frac{S_{aa(1)}}{K_{s,aa} + S_{aa(1)}} * X_{aa(1)} * I_1 \right) + (1 - Y_{c4})0.3 * \left(k_{fa} * \frac{S_{fa(1)}}{K_{s,fa} + S_{fa(1)}} * X_{fa(1)} * I_2 \right) + (1 - Y_{c4})0.15$$
$$* \left(k_{c4} * \frac{S_{va(1)}}{K_{s,c4} + S_{va(1)}} * X_{c4(1)} * \frac{S_{va(1)}}{S_{va(1)} + S_{bu(1)}} * I_2 \right) + (1 - Y_{c4})0.2$$
$$* \left(k_{c4} * \frac{S_{bu(1)}}{K_{s,c4} + S_{bu(1)}} * X_{c4(1)} * \frac{S_{bu(1)}}{S_{va(1)} + S_{bu(1)}} * I_2 \right) + (1 - Y_{pro})0.43$$
$$\left. * \left(k_{pro} * \frac{S_{pro(1)}}{K_{s,pro} + S_{pro(1)}} * X_{pro(1)} * I_2 \right) - \left(k_{h2} * \frac{S_{h2(1)}}{K_{s,h2} + S_{h2(1)}} * X_{h2(1)} * I_1' \right) \right]$$

$$\boldsymbol{S_{h2(1)} = \frac{S_{h2(0)} + \Delta t * \left(\begin{array}{c} (1 - Y_{su}) * f_{h2,su} * \left(k_{su} * \frac{S_{su(1)}}{K_{s,su} + S_{su(1)}} * X_{su(1)} * I_{ph1} I_{IN,\lim} \right) \\ +(1 - Y_{aa}) * f_{h2,aa} * \left(k_{aa} * \frac{S_{aa(1)}}{K_{s,aa} + S_{aa(1)}} * X_{aa(1)} * I_{ph1} I_{IN,\lim} \right) \\ +(1 - Y_{c4})0.3 * \left(k_{fa} * \frac{S_{fa(1)}}{K_{s,fa} + S_{fa(1)}} * X_{fa(1)} * I_{ph1} I_{IN,\lim} \frac{K_{Ih2fa}}{K_{Ih2fa} + S_{h2(1)}} \right) \\ +(1 - Y_{c4})0.15 * \left(k_{c4} * \frac{S_{va(1)}}{K_{s,c4} + S_{va(1)}} * X_{c4(1)} * \frac{S_{va(1)}}{S_{va(1)} + S_{bu(1)}} * I_{ph1} I_{IN,\lim} \frac{K_{Ih2c4}}{K_{Ih2c4} + S_{h2(1)}} \right) \\ +(1 - Y_{c4})0.2 * \left(k_{c4} * \frac{S_{bu(1)}}{K_{s,c4} + S_{bu(1)}} * X_{c4(1)} * \frac{S_{bu(1)}}{S_{va(1)} + S_{bu(1)}} * I_{ph1} I_{IN,\lim} \frac{K_{Ih2c4}}{K_{Ih2c4} + S_{h2(1)}} \right) \\ +(1 - Y_{pro})0.43 * \left(k_{pro} * \frac{S_{pro(1)}}{K_{s,pro} + S_{pro(1)}} * X_{pro(1)} * I_{ph1} I_{IN,\lim} \frac{K_{Ih2pro}}{K_{Ih2pro} + S_{h2(1)}} \right) \end{array} \right)}{1 + \Delta t * \left(k_{h2} * \frac{1}{K_{s,h2} + S_{h2(1)}} * X_{h2(1)} * I_{ph3} I_{IN,\lim} I_{NH,Xh2} I_{HAC,Xh2} \right)}}$$

A. 9 Mass balance on methane gas S_{ch4}

$$V * \left(\frac{dS_{ch4}}{dt}\right) = Q * S_{ch4,in} - Q * S_{ch4} + V * [(1 - Y_{ac}) * r'_{11} + (1 - Y_{h2}) * r'_{12}]$$

$$V * \left(\frac{dS_{ch4}}{dt}\right) = Q * S_{ch4,in} - Q * S_{ch4} + V * \left[(1 - Y_{ac}) * \left(k_{ac} * \frac{S_{ac}}{K_{s,ac} + S_{ac} \Big/ \frac{S_{ac(1)}^2}{K_{IAC,Xac}}} * X_{ac} * I'_3\right) + (1 - Y_{h2}) * \left(k_{h2} * \frac{S_{h2}}{K_{s,h2} + S_{h2}} * X_{h2} * I'_1\right)\right]$$

$$V * \left(\frac{dS_{ch4}}{dt}\right) = V * \left[(1 - Y_{ac}) * \left(k_{ac} * \frac{S_{ac}}{K_{s,ac} + S_{ac} + \frac{S_{ac(1)}^2}{K_{IAC,Xac}}} * X_{ac} * I'_3\right) + (1 - Y_{h2}) * \left(k_{h2} * \frac{S_{h2}}{K_{s,h2} + S_{h2}} * X_{h2} * I'_1\right)\right]$$

$$\boldsymbol{S_{ch4(1)} = S_{ch4(0)} + \Delta t * \left((1 - Y_{ac}) * \left(k_{ac} * \frac{S_{ac(1)}}{K_{s,ac} + S_{ac(1)} + \frac{S_{ac(1)}^2}{K_{IAC,Xac}}} * X_{ac(1)} * I_{ph2} I_{IN,\lim} I_{NH,Xac} I_{HAC,Xac}\right) + (1 - Y_{h2}) * \left(k_{h2} * \frac{S_{h2(1)}}{K_{s,h2} + S_{h2(1)}} * X_{h2(1)} * I_{ph3} I_{IN,\lim} I_{NH,Xh2} I_{HAC,Xh2}\right)\right)}$$

Particulate Components

A. 10 Mass balance on particulate composites X_c

$$V * \left(\frac{dX_c}{dt}\right) = Q * X_{c,in} - Q * X_c + V * [r_{13} + r_{14} + r_{15} + r_{16} + r_{17} + r_{18} + r_{19} - r_1]$$

$$V * \left(\frac{dX_c}{dt}\right) = Q * X_{c,in} - Q * X_c + V * \left[k_{dec,Xsu}X_{su} + k_{dec,Xaa}X_{aa} + k_{dec,Xfa}X_{fa} + k_{dec,Xc4}X_{c4} + k_{dec,Xpro}X_{pro} + k_{dec,Xac}X_{ac} + k_{dec,Xh2}X_{h2} - k_{dis}X_c\right]$$

$$V * \left(\frac{dX_c}{dt}\right) = V * \left[k_{dec,Xsu}X_{su} + k_{dec,Xaa}X_{aa} + k_{dec,Xfa}X_{fa} + k_{dec,Xc4}X_{c4} + k_{dec,Xpro}X_{pro} + k_{dec,Xac}X_{ac} + k_{dec,Xh2}X_{h2} - k_{dis}X_c\right]$$

$$X_{c(1)} = X_{c(0)} + \Delta t * \left[k_{dec,Xsu}X_{su(1)} + k_{dec,Xaa}X_{aa(1)} + k_{dec,Xfa}X_{fa(1)} + k_{dec,Xc4}X_{c4(1)} + k_{dec,Xpro}X_{pro(1)} + k_{dec,Xac}X_{ac(1)} + k_{dec,Xh2}X_{h2(1)} - k_{dis}X_{c(1)}\right]$$

$$\boldsymbol{X_{c(1)} = \frac{X_{c(0)} + \Delta t * \begin{pmatrix} k_{dec,Xsu}X_{su(1)} + k_{dec,Xaa}X_{aa(1)} \\ +k_{dec,Xfa}X_{fa(1)} + k_{dec,Xc4}X_{c4(1)} \\ +k_{dec,Xpro}X_{pro(1)} + k_{dec,Xac}X_{ac(1)} + k_{dec,Xh2}X_{h2(1)} \end{pmatrix}}{1 + \Delta t * k_{dis}}}$$

A. 11 Mass balance on particulate carbohydrates X_{ch}

$$V * \left(\frac{dX_{ch}}{dt}\right) = Q * X_{ch,in} - Q * X_{ch} + V * \left[f_{ch,xc} * r_1 - r_2\right]$$

$$V * \left(\frac{dX_{ch}}{dt}\right) = Q * X_{ch,in} - Q * X_{ch} + V * \left[f_{ch,xc} * k_{dis} X_c - k_{hyd,ch} X_{ch}\right]$$

$$V * \left(\frac{dX_{ch}}{dt}\right) = V * \left[f_{ch,xc} * k_{dis} X_c - k_{hyd,ch} X_{ch}\right]$$

$$X_{ch(1)} = X_{ch(0)} + \Delta t * \left[f_{ch,xc} * k_{dis} X_{c(1)} - k_{hyd,ch} X_{ch(1)}\right]$$

$$\boldsymbol{X_{ch(1)} = \frac{X_{ch(0)} + \Delta t * \left[f_{ch,xc} * k_{dis} X_{c(1)}\right]}{1 + \Delta t * k_{hyd,ch}}}$$

A. 12 Mass balance on particulate protein X_{pr}

$$V * \left(\frac{dX_{pr}}{dt}\right) = Q * X_{pr,in} - Q * X_{pr} + V * \left[f_{pr,xc} * r_1 - r_3\right]$$

$$V * \left(\frac{dX_{pr}}{dt}\right) = Q * X_{pr,in} - Q * X_{pr} + V * \left[f_{pr,xc} * k_{dis} X_c - k_{hyd,pr} X_{pr}\right]$$

$$V * \left(\frac{dX_{pr}}{dt}\right) = V * \left[f_{pr,xc} * k_{dis} X_c - k_{hyd,pr} X_{pr}\right]$$

$$X_{pr(1)} = X_{pr(0)} + \Delta t * \left[f_{pr,xc} * k_{dis} X_{c(1)} - k_{hyd,pr} X_{pr(1)}\right]$$

$$\boldsymbol{X_{pr(1)} = \frac{X_{pr(0)} + \Delta t * \left[f_{pr,xc} * k_{dis} X_{c(1)}\right]}{1 + \Delta t * k_{hyd,pr}}}$$

A. 13 Mass balance on particulate lipids X_{li}

$$V * \left(\frac{dX_{li}}{dt}\right) = Q * X_{li,in} - Q * X_{li} + V * \left[f_{li,xc} * r_1 - r_4\right]$$

$$V * \left(\frac{dX_{li}}{dt}\right) = Q * X_{li,in} - Q * X_{li} + V * \left[f_{li,xc} * k_{dis} X_c - k_{hyd,Xli} X_{li}\right]$$

$$V * \left(\frac{dX_{li}}{dt}\right) = V * \left[f_{li,xc} * k_{dis} X_c - k_{hyd,Xli} X_{li}\right]$$

$$X_{li(1)} = X_{li(0)} + \Delta t * \left[f_{li,xc} * k_{dis} X_{c(1)} - k_{hyd,Xli} X_{li(1)}\right]$$

$$\boldsymbol{X_{li(1)} = \frac{X_{li(0)} + \Delta t * \left[f_{li,xc} * k_{dis} X_{c(1)}\right]}{1 + \Delta t * k_{hyd,Xli}}}$$

A. 14 Mass balance on sugar degraders X_{su}

$$V * \left(\frac{dX_{su}}{dt}\right) = Q * X_{su,in} - Q * X_{su} + V * \left[Y_{su} * r_5 - r_{13}\right]$$

$$V * \left(\frac{dX_{su}}{dt}\right) = Q * X_{su,in} - Q * X_{su} + V * \left[Y_{su} * \left(k_{su} * \frac{S_{su}}{K_{s,su} + S_{su}} * X_{su} * I_1\right) - k_{dec,Xsu} X_{su}\right]$$

$$V * \left(\frac{dX_{su}}{dt}\right) = V * \left[Y_{su} * \left(k_{su} * \frac{S_{su}}{K_{s,su} + S_{su}} * X_{su} * I_1\right) - k_{dec,Xsu} X_{su}\right]$$

$$X_{su(1)} = X_{su(0)} + \Delta t * \left[Y_{su} * \left(k_{su} * \frac{S_{su(1)}}{K_{s,su} + S_{su(1)}} * X_{su(1)} * I_1\right) - k_{dec,Xsu} X_{su(1)}\right]$$

$$\boldsymbol{X_{su(1)} = \frac{X_{su(0)}}{1 + \Delta t * [k_{dec,Xsu} - Y_{su} * \left(k_{su} * \frac{S_{su(1)}}{K_{s,su} + S_{su(1)}} * I_{ph1} I_{IN,\text{lim}}\right)]}}$$

A. 15 Mass balance on amino acid degraders X_{aa}

$$V * \left(\frac{dX_{aa}}{dt}\right) = Q * X_{aa,in} - Q * X_{aa} + V * [Y_{aa} * r_6 - r_{14}]$$

$$V * \left(\frac{dX_{aa}}{dt}\right) = Q * X_{aa,in} - Q * X_{aa} + V * \left[Y_{aa} * \left(k_{aa} * \frac{S_{aa}}{K_{s,aa} + S_{aa}} * X_{aa} * I_1\right) - k_{dec,Xaa} X_{aa}\right]$$

$$V * \left(\frac{dX_{aa}}{dt}\right) = V * \left[Y_{aa} * \left(k_{aa} * \frac{S_{aa}}{K_{s,aa} + S_{aa}} * X_{aa} * I_1\right) - k_{dec,Xaa} X_{aa}\right]$$

$$X_{aa(1)} = X_{aa(0)} + \Delta t * \left[Y_{aa} * \left(k_{aa} * \frac{S_{aa(1)}}{K_{s,aa} + S_{aa(1)}} * X_{aa(1)} * I_1\right) - k_{dec,Xaa} X_{aa(1)}\right]$$

$$\boldsymbol{X_{aa(1)} = \frac{X_{aa(0)}}{1 + \Delta t * \left[k_{dec,Xaa} - Y_{aa} * \left(k_{aa} * \frac{S_{aa(1)}}{K_{s,aa} + S_{aa(1)}} * I_{ph} I_{IN,\text{lim}}\right)\right]}}$$

A. 16 Mass balance on LCFA degraders X_{fa}

$$V * \left(\frac{dX_{fa}}{dt}\right) = Q * X_{fa,in} - Q * X_{fa} + V * [Y_{fa} * r_7 - r_{15}]$$

$$V * \left(\frac{dX_{fa}}{dt}\right) = Q * X_{fa,in} - Q * X_{fa} + V * \left[Y_{fa} * \left(k_{fa} * \frac{S_{fa}}{K_{s,fa} + S_{fa}} * X_{fa} * I_2\right) - k_{dec,Xfa} X_{fa}\right]$$

$$V * \left(\frac{dX_{fa}}{dt}\right) = V * \left[Y_{fa} * \left(k_{fa} * \frac{S_{fa}}{K_{s,fa} + S_{fa}} * X_{fa} * I_2\right) - k_{dec,Xfa} X_{fa}\right]$$

$$X_{fa(1)} = X_{fa(0)} + \Delta t * \left[Y_{fa} * \left(k_{fa} * \frac{S_{fa(1)}}{K_{s,fa} + S_{fa(1)}} * X_{fa(1)} * I_2 \right) - k_{dec,Xfa} X_{fa(1)} \right]$$

$$\boldsymbol{X_{fa(1)} = \frac{X_{fa(0)}}{1 + \Delta t * \left[k_{dec,Xfa} - Y_{fa} * \left(k_{fa} * \frac{S_{fa(1)}}{K_{s,fa} + S_{fa(1)}} * I_{ph1} I_{IN,\lim} \frac{K_{Ih2fa}}{K_{Ih2fa} + S_{h2(1)}} \right) \right]}}$$

A. 17 Mass balance on butyrate degraders X_{c4}

$$V * \left(\frac{dX_{c4}}{dt} \right) = Q * X_{c4,in} - Q * X_{c4} + V * [Y_{c4} * r_8 + Y_{c4} * r_9 - r_{16}]$$

$$V * \left(\frac{dX_{c4}}{dt} \right) = Q * X_{c4,in} - Q * X_{c4} + V * \left[Y_{c4} * \left(k_{c4} * \frac{S_{va}}{K_{s,c4} + S_{va}} * X_{c4} * \frac{S_{va}}{S_{va} + S_{bu}} * I_2 \right) + Y_{c4} * \left(k_{c4} * \frac{S_{bu}}{K_{s,c4} + S_{bu}} * X_{c4} * \frac{S_{bu}}{S_{va} + S_{bu}} * I_2 \right) - k_{dec,Xc4} X_{c4} \right]$$

$$V * \left(\frac{dX_{c4}}{dt} \right) = V * \left[Y_{c4} * \left(k_{c4} * \frac{S_{va}}{K_{s,c4} + S_{va}} * X_{c4} * \frac{S_{va}}{S_{va} + S_{bu}} * I_2 \right) + Y_{c4} * \left(k_{c4} * \frac{S_{bu}}{K_{s,c4} + S_{bu}} * X_{c4} * \frac{S_{bu}}{S_{va} + S_{bu}} * I_2 \right) - k_{dec,Xc4} X_{c4} \right]$$

$$X_{c4(1)} = X_{c4(0)} + \Delta t * \left[Y_{c4} * \left(k_{c4} * \frac{S_{va(1)}}{K_{s,c4} + S_{va(1)}} * X_{c4(1)} * \frac{S_{va(1)}}{S_{va(1)} + S_{bu(1)}} * I_2 \right) + Y_{c4} * \left(k_{c4} * \frac{S_{bu(1)}}{K_{s,c4} + S_{bu(1)}} * X_{c4(1)} * \frac{S_{bu(1)}}{S_{va(1)} + S_{bu(1)}} * I_2 \right) - k_{dec,Xc4} X_{c4(1)} \right]$$

$$\boldsymbol{X_{c4(1)} = \frac{X_{c4(0)}}{1 + \Delta t * \left(\begin{array}{l} k_{dec,Xc4} - Y_{c4} * k_{c4} * I_{ph1} I_{IN,\lim} \frac{K_{Ih2c4}}{K_{Ih2c4} + S_{h2(1)}} * \left(\frac{S_{va(1)}}{K_{s,c4} + S_{va(1)}} * \frac{S_{va(1)}}{S_{va(1)} + S_{bu(1)}} \right) \\ + Y_{c4} * k_{c4} * I_{ph1} I_{IN,\lim} \frac{K_{Ih2c4}}{K_{Ih2c4} + S_{h2(1)}} * \left(\frac{S_{bu(1)}}{K_{s,c4} + S_{bu(1)}} * \frac{S_{bu(1)}}{S_{va(1)} + S_{bu(1)}} \right) \end{array} \right)}}$$

A. 18 Mass balance on propionate degraders X_{pro}

$$V * \left(\frac{dX_{pro}}{dt} \right) = Q * X_{pro,in} - Q * X_{pro} + V * \left[Y_{pro} * r_{10} - r_{17} \right]$$

$$V * \left(\frac{dX_{pro}}{dt} \right) = Q * X_{pro,in} - Q * X_{pro} + V * \left[Y_{pro} * \left(k_{pro} * \frac{S_{pro}}{K_{s,pro} + S_{pro}} * X_{pro} * I_2 \right) - k_{dec,Xpro} X_{pro} \right]$$

$$V * \left(\frac{dX_{pro}}{dt} \right) = V * \left[Y_{pro} * \left(k_{pro} * \frac{S_{pro}}{K_{s,pro} + S_{pro}} * X_{pro} * I_2 \right) - k_{dec,Xpro} X_{pro} \right]$$

$$X_{pro(1)} = X_{pro(0)} + \Delta t * \left[Y_{pro} * \left(k_{pro} * \frac{S_{pro(1)}}{K_{s,pro} + S_{pro(1)}} * X_{pro(1)} * I_2 \right) - k_{dec,Xpro} X_{pro(1)} \right]$$

$$\boldsymbol{X_{pro(1)} = \frac{X_{pro(0)}}{1 + \Delta t * \left[k_{dec,Xpro} - Y_{pro} * \left(k_{pro} * \frac{S_{pro(1)}}{K_{s,pro} + S_{pro(1)}} * I_{ph1} I_{IN,\lim} \frac{K_{Ih2pro}}{K_{Ih2pro} + S_{h2(1)}} \right) \right]}}$$

A. 19 Mass balance on acetoclastic methanogens X_{ac}

$$V * \left(\frac{dX_{ac}}{dt}\right) = Q * X_{ac,in} - Q * X_{ac} + V * [Y_{ac} * r'_{11} - r_{18}]$$

$$V * \left(\frac{dX_{ac}}{dt}\right) = Q * X_{ac,in} - Q * X_{ac} + V * \left[Y_{ac} * \left(k_{ac} * \frac{S_{ac}}{K_{s,ac} + S_{ac}} * X_{ac} * I'_3\right) - k_{dec,Xac} X_{ac}\right]$$

$$V * \left(\frac{dX_{ac}}{dt}\right) = V * \left[Y_{ac} * \left(k_{ac} * \frac{S_{ac}}{K_{s,ac} + S_{ac}} * X_{ac} * I'_3\right) - k_{dec,Xac} X_{ac}\right]$$

$$X_{ac(1)} = X_{ac(0)} + \Delta t * \left[Y_{ac} * \left(k_{ac} * \frac{S_{ac(1)}}{K_{s,ac} + S_{ac(1)} + {S_{ac(1)}^2}/{K_{IAC,Xac}}} * X_{ac(1)} * I'_3\right) - k_{dec,Xac} X_{ac(1)}\right]$$

$$\boldsymbol{X_{ac(1)} = \frac{X_{ac(0)}}{1 + \Delta t * \left[k_{dec,Xac} - Y_{ac} * \left(k_{ac} * \frac{S_{ac(1)}}{K_{s,ac} + S_{ac(1)} + {S_{ac(1)}^2}/{K_{IAC,Xac}}} * I_{ph2} I_{IN,\lim} I_{NH,Xac} I_{HAC,Xac}\right)\right]}}$$

A. 20 Mass balance on hydrogenotrophic methanogens X_{h2}

$$V * \left(\frac{dX_{h2}}{dt}\right) = Q * X_{h2,in} - Q * X_{h2} + V * [Y_{h2} * r'_{12} - r_{19}]$$

$$V * \left(\frac{dX_{h2}}{dt}\right) = Q * X_{h2,in} - Q * X_{h2} + V * \left[Y_{h2} * \left(k_{h2} * \frac{S_{h2}}{K_{s,h2} + S_{h2}} * X_{h2} * I'_1\right) - k_{dec,Xh2} X_{h2}\right]$$

$$V * \left(\frac{dX_{h2}}{dt}\right) = V * \left[Y_{h2} * \left(k_{h2} * \frac{S_{h2}}{K_{s,h2} + S_{h2}} * X_{h2} * I'_1\right) - k_{dec,Xh2} X_{h2}\right]$$

$$X_{h2(1)} = X_{h2(0)} + \Delta t * \left[Y_{h2} * \left(k_{h2} * \frac{S_{h2(1)}}{K_{s,h2} + S_{h2(1)}} * X_{h2(1)} * I_1' \right) - k_{dec,Xh2} X_{h2(1)} \right]$$

$$\boldsymbol{X_{h2(1)} = \frac{X_{h2(0)}}{1 + \Delta t * \left[k_{dec,Xh2} - Y_{h2} * \left(k_{h2} * \frac{S_{h2(1)}}{K_{s,h2} + S_{h2(1)}} * I_{ph3} I_{IN,\lim} I_{NH,Xh2} I_{HAC,Xh2} \right) \right]}}$$

A. 21 Mass balance on particulate inert solids X_i

$$V * \left(\frac{dX_i}{dt} \right) = Q * X_{i,in} - Q * X_i + V * \left[f_{i,xc} * r_1 \right]$$

$$V * \left(\frac{dX_i}{dt} \right) = Q * X_{i,in} - Q * X_i + V * \left[f_{i,xc} * k_{dis} X_c \right]$$

$$V * \left(\frac{dX_i}{dt} \right) = V * \left[f_{i,xc} * k_{dis} X_c \right]$$

$$\boldsymbol{X_{i(1)} = X_{i(0)} + \Delta t * \left[f_{i,xc} * k_{dis} X_{c(1)} \right]}$$

Appendix B: Additional Information

Table B.1: Further characterization of sludge (analogous to Table 2.1) for BMP test operated at 37.5 ºC.

	Inoculum	TWAS
Volume (mL)	20	50
TCOD (g/L)	26.0 ± 0.4	43.9 ± 0.3
sCOD (g/L)	1.3 ± 0.1	4.8 ± 0.1
TSS (g/L)	32.3 ± 3.7	36.2 ± 0.1
VSS (g/L)	19.0 ± 1.2	27.3 ± 0.1
TAN (mg-N/L)	2.4 ± 0.4	303 ± 36
pH	7.7 ± 0.0	6.7 ± 0.3

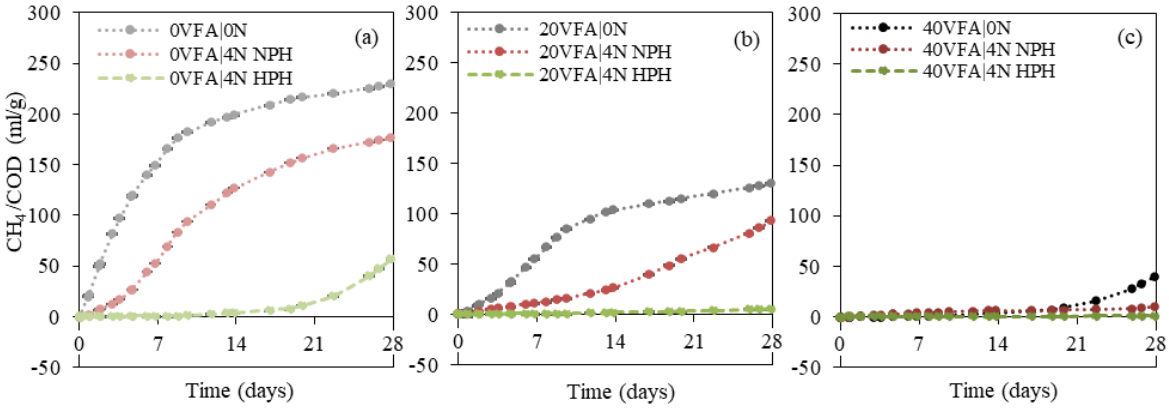

Figure B.1: Normalized methane production curves from BMP experimental tests for initial substrate (g-COD) for: (a) 0VFA conditions, (b) 20VFA conditions, and (c) 40VFA conditions.